







ABRO1 promotes NLRP3 inflammasome activation through regulation of NLRP3 deubiquitination

Guangming Ren¹ , Xuanyi Zhang¹ , Yang Xiao¹ , Wen Zhang^{1,2}, Yu Wang^{1,3}, Wenbing Ma¹, Xiaohan Wang¹, Pan Song⁴, Lili Lai⁴, Hui Chen¹, Yiqun Zhan¹, Jianhong Zhang^{1,5}, Miao Yu¹ , Changhui Ge⁴, Changyan Li¹ , Ronghua Yin^{1,*}  & Xiaoming Yang^{1,2,**}

Abstract

Deubiquitination of NLRP3 has been suggested to contribute to inflammasome activation, but the roles and molecular mechanisms are still unclear. We here demonstrate that ABRO1, a subunit of the BRISC deubiquitinase complex, is necessary for optimal NLRP3-ASC complex formation, ASC oligomerization, caspase-1 activation, and IL-1 β and IL-18 production upon treatment with NLRP3 ligands after the priming step, indicating that efficient NLRP3 activation requires ABRO1. Moreover, we report that ABRO1 deficiency results in a remarkable attenuation in the syndrome severity of NLRP3-associated inflammatory diseases, including MSU- and Alum-induced peritonitis and LPS-induced sepsis in mice. Mechanistic studies reveal that LPS priming induces ABRO1 binding to NLRP3 in an S194 phosphorylation-dependent manner, subsequently recruiting the BRISC to remove K63-linked ubiquitin chains of NLRP3 upon stimulation with activators. Furthermore, deficiency of BRCC3, the catalytically active component of BRISC, displays similar phenotypes to ABRO1 knockout mice. Our findings reveal an ABRO1-mediated regulatory signaling system that controls activation of the NLRP3 inflammasome and provide novel potential targets for treating NLRP3-associated inflammatory diseases.

Keywords ABRO1; BRCC3; deubiquitination; NLRP3 inflammasome; phosphorylation

Subject Categories Immunology; Microbiology, Virology & Host Pathogen Interaction

DOI 10.15252/emboj.2018100376 | Received 30 July 2018 | Revised 13 January 2019 | Accepted 18 January 2019 | Published online 20 February 2019

The EMBO Journal (2019) 38: e100376

Introduction

The NOD-like receptor family protein 3 (NLRP3) inflammasome is a critical component of innate immunity (Schroder & Tschopp, 2010).

It is capable of sensing cellular stress derived from a wide variety of stimuli, including invading pathogens, pore-forming toxins, endogenous danger signals, metabolic dysfunction, and pollutant particles (Abderrazak *et al*, 2015). Consequently, dysregulated NLRP3 inflammasome activation is associated with both heritable and acquired inflammatory diseases (Menu & Vince, 2011; de Torre-Minguela *et al*, 2017).

Successful NLRP3 inflammasome activation requires two sequential steps: priming and activation (He *et al*, 2016). The key priming event is the NF- κ B-mediated transcription of pro-IL-1 β and NLRP3 (Bauernfeind *et al*, 2009). The following activation step is characterized by the assembly of the NLRP3 inflammasome complex and the subsequent proteolytic processing of pro-IL-1 β and pro-IL-18 by autocatalytically activated pro-caspase-1. The regulation of NLRP3 inflammasome activation has been extensively investigated. A number of studies have reported that regulation of NLRP3 inflammasome activity occurs by modification of NLRP3 at the transcription level (Fernandes-Alnemri *et al*, 2013; Huai *et al*, 2014). Nonetheless, accumulating evidence also indicates that post-translational modifications (PTMs; Baker *et al*, 2017), especially ubiquitination and phosphorylation, modulate NLRP3 and ASC (apoptosis-associated speck-like protein containing a CARD) to facilitate the assembly of inflammasome complexes, which are controlled by protein turnover (Yan *et al*, 2015b), protein distribution and location (Subramanian *et al*, 2013), and the intricate protein–protein interactions (Stutz *et al*, 2017).

It has been reported that NLRP3 is poly-ubiquitinated in resting macrophages with mixed Lys-48 and Lys-63 ubiquitin chains (Juliana *et al*, 2012; Py *et al*, 2013). Lys48-linked polyubiquitin plays a major role in NLRP3 stability. Several E3 ubiquitin ligases, such as MARCH7 (Yan *et al*, 2015b), TRIM31 (Song *et al*, 2016), and FBXL2 (Han *et al*, 2015), have been shown to promote Lys48-linked ubiquitination of NLRP3, leading to its degradation (Baker *et al*, 2017). In addition, previous studies have shown that an additional decrease in ubiquitinated NLRP3 can be induced by inflammasome activation signals (Juliana *et al*, 2012). Inhibition of

1 State Key Laboratory of Proteomics, Beijing Proteome Research Center, National Center for Protein Sciences (Beijing), Beijing Institute of Lifeomics, Beijing, China

2 Department of Pharmaceutical Engineering, School of Chemical Engineering and Technology, Tianjin University, Tianjin, China

3 An Hui Medical University, Hefei, China

4 Beijing Institute of Radiation Medicine, Beijing, China

5 Institute for Immunology and School of Medicine, Tsinghua University, Beijing, China

*Corresponding author. Tel: +86 10 66930293; E-mail: yrh1980110@126.com

**Corresponding author. Tel: +86 10 61777000; E-mail: xiaomingyang@sina.com

NLRP3 deubiquitination by pharmacologic administration of nonspecific DUB inhibitors almost completely blocks NLRP3 activation in both mouse and human cells (Juliana *et al*, 2012; Lopez-Castejon *et al*, 2013), indicating that deubiquitination is required not only for NLRP3 stability but also for NLRP3 inflammasome activation. Subsequently, the deubiquitination enzyme BRCA1/BRCA2-containing complex subunit 3 (BRCC3, also known as BRCC36 in human) is identified as a critical regulator of NLRP3 ubiquitination and inflammasome activity by knockdown experiments *in vitro* (Py *et al*, 2013). However, the *in vivo* role of the BRCC3 in NLRP3 deubiquitination and the underlying molecular mechanisms are still unknown. Moreover, a previous study has reported that mice lacking Abraxas brother 1 (ABRO1, also known as Abraxas 2 and KIAA0157), a scaffold to assemble the BRCC3 complex (also known as BRCC36 isopeptidase complex [BRISC]), exhibit a markedly decreased severity of LPS-induced injury and display significantly reduced mortality, which indicates that BRCC3 complex is an important regulator of cellular responses to LPS (Zheng *et al*, 2013). LPS-induced inflammatory cytokines including interleukin 1-beta (IL-1 β) and IL-18 play a key role in LPS-induced septic shock. Neutralization of IL-1 and IL-18, using the IL-1 receptor antagonist anakinra and anti-IL-18 antibodies, conferred complete protection against endotoxin-induced lethality (Vanden Berghe *et al*, 2014). However, Zheng *et al* (2013) have shown that ABRO1 knockout results in a decreased induction of *Il1b* mRNA in blood leukocytes by LPS treatment, and LPS plus ATP-induced caspase-1 activation is not impaired in *Abro1*^{-/-} macrophages. As ABRO1 is an important subunit of the BRCC3 complex, and removal of ABRO1 leads to the loss of BRCC3 deubiquitinase (DUB) activity (Feng *et al*, 2010), these results imply that the BRCC3 complex probably does not contribute to NLRP3 inflammasome activation upon LPS plus ATP challenge (Zheng *et al*, 2013). Thus, the role of the BRCC3 complex in the NLRP3 inflammasome is controversial, and further studies are required to clarify the contribution of BRCC3 complex to NLRP3 inflammasome activation.

BRCC3 is a JAB1/MPN/Mov34 (JAMM) domain-containing Zn²⁺ metalloprotease DUB (Cooper *et al*, 2009). In the cytoplasm, BRCC3 forms a multiprotein complex (BRISC) with ABRO1, NBA1, and BRE that specifically cleaves “Lys(K)-63”-linked ubiquitin (Feng *et al*, 2010). ABRO1 is a paralog of a BRCA1-interacting protein, Abraxas, and they share 39% sequence homology within their amino-terminal regions (Wang *et al*, 2007). ABRO1 contains a structural domain that interacts with subunits NBA1, BRE, and BRCC36 (Hu *et al*, 2011) but lacks the PSXXF domain that serves as a specific recognition motif for the BRCT domain of BRCA1 (Wang *et al*, 2007). Therefore, ABRO1 does not interact with BRCA1 but serves as a scaffold protein and recruits the rest of the components, including NBA1, BRE, and BRCC3, to form the BRISC (Feng *et al*, 2010). So far, only a few substrates of BRISC have been identified, including the type 1 interferon (IFN) receptor chain 1 (IFNAR1) (Zheng *et al*, 2013), the essential spindle assembly factor nuclear mitotic apparatus (NuMA) (Yan *et al*, 2015a), the poly (ADP-ribose) polymerase tankyrase 1 (Tripathi & Smith, 2017), and the HIV-1 Tat protein (Xu *et al*, 2018).

Here, we describe a specific function of ABRO1 as a regulator of the NLRP3 inflammasome complex in macrophages. Our results generate a model involving that LPS priming induces ABRO1 binding to NLRP3 in an S194 phosphorylation-dependent manner,

leading to ABRO1-dependent recruitment of BRISC which mediates deubiquitination of NLRP3 upon inflammasome activation. Importantly, we provide clear genetic evidence from knockout mice that BRISC plays a key role in the regulation of NLRP3 inflammasome.

Results

***Abro1*^{-/-} macrophages show specific defective activation of the NLRP3 inflammasome**

To further investigate the potential functions of ABRO1, we generated *Abro1*-deficient (*Abro1*^{-/-}) mice by the partial deletion of exon 1 of the murine *Abro1* locus (Fig EV1A and B). In line with a previous report, *Abro1*^{-/-} mice appeared normal and showed no anatomical abnormalities (Zheng *et al*, 2013). Based on the observation that *Abro1*^{-/-} mice and cells display abnormalities in response to LPS stimulation (Zheng *et al*, 2013), we investigated the role of ABRO1 in macrophages. The development and proliferation abilities were comparable between *Abro1*^{+/+} and *Abro1*^{-/-} bone marrow-derived macrophages (BMDMs; Fig EV1C and D). LPS-induced production of IL-6 and TNF- α in condition medium was comparable between *Abro1*^{+/+} and *Abro1*^{-/-} BMDMs (Fig EV1E). However, *Abro1*^{-/-} BMDMs generated significantly less IL-1 β and IL-18 compared with *Abro1*^{+/+} BMDMs in response to LPS priming and ATP stimulation (Fig 1A and B). ABRO1 overexpression greatly enhanced IL-1 β secretion in *Abro1*^{+/+} BMDMs, and re-expression of exogenous ABRO1 protein in *Abro1*^{-/-} macrophages restored IL-1 β secretion to a similar level observed in *Abro1*^{+/+} cells in response to inflammasome activation (Fig 1C). Moreover, knockdown of ABRO1 significantly reduced IL-1 β release in human monocyte-derived macrophages (HMDMs) treated with LPS plus ATP (Fig 1D). Similarly, significant decreases of IL-1 β production were also observed in response to other NLRP3 inflammasome stimuli, including nigericin, silica, monosodium urate crystals (MSU), muramyl dipeptide (MDP), and aluminum (Alum) in *Abro1*^{-/-} macrophages (Fig 1E). These results indicate that activation of the NLRP3 inflammasome is defective in *Abro1*^{-/-} macrophages. Importantly, IL-1 β defects in *Abro1*^{-/-} BMDMs were not due to altered inflammasome-related core protein levels (Fig EV1F), LPS unresponsiveness (depicted by LPS/TLR4 signaling pathway activation, *Il1b*, *Tnfa*, and *Il6* transcript expression levels, TNF- α , and IL-6 release; Fig EV1G, H, and E), nor reduced macrophage viability (Fig EV1I). Of note, *Nlrp3*^{-/-} BMDMs showed almost a complete loss of IL-1 β release, while the IL-1 β release is generally only reduced by about 70% in *Abro1*^{-/-} BMDMs relative to wild-type cells after LPS plus ATP or LPS plus nigericin treatment (Fig EV2A). Therefore, our results suggest that ABRO1 is required for effective activation of the NLRP3 inflammasome and IL-1 β secretion upon stimulation with the NLRP3 ligands.

We next investigated whether ABRO1 was important for the activation of other inflammasomes, namely the NLRP1 (activated with anthrax lethal toxin), NLRC4 (activated with *Salmonella* flagellin), and AIM2 (activated with poly(dA:dT)) inflammasomes (Baroja-Mazo *et al*, 2014). As shown in Fig 1E, *Abro1*^{-/-} and *Abro1*^{+/+} BMDMs generated comparable levels of IL-1 β in response to anthrax lethal toxin (LTx), flagellin and poly(dA:dT), indicating that ABRO1 is specific for NLRP3 inflammasome activation.

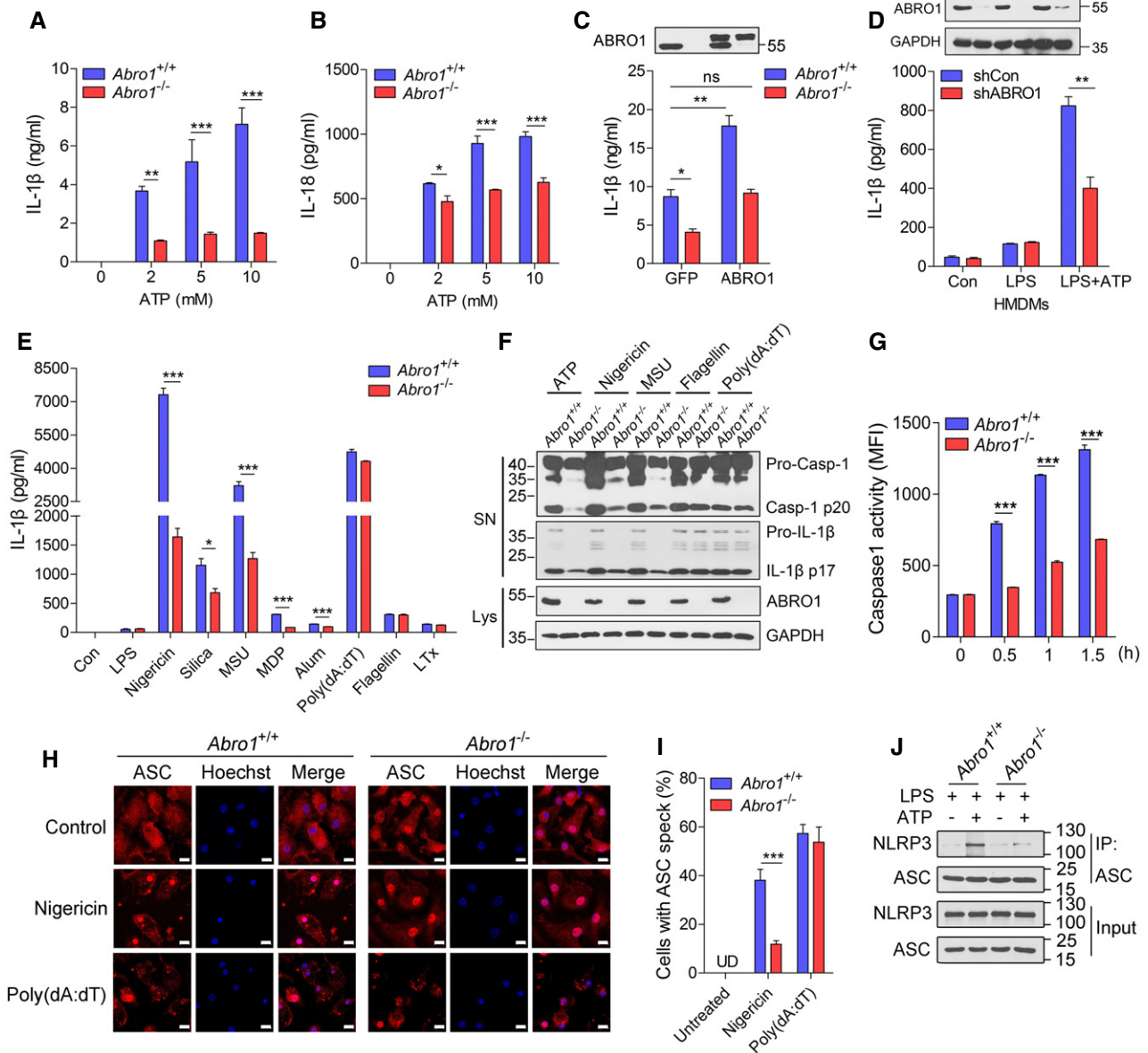


Figure 1. *Abro1*^{-/-} macrophages show defective activation of the NLRP3 inflammasome.

A, B LPS-primed *Abro1*^{+/+} and *Abro1*^{-/-} BMDMs were treated with various doses of ATP. CBA analysis of IL-1 β (A) and ELISA of IL-18 (B) in the culture supernatants.

C CBA analysis of IL-1 β secretion from *Abro1*^{+/+} and *Abro1*^{-/-} BMDMs transduced with GFP- or ABRO1-GFP-expressing lentiviruses prior to stimulation with LPS and ATP. Cell lysates were immunoblotted with anti-ABRO1 antibody.

D ELISA analysis of IL-1 β secretion from HMDMs transduced with lentiviruses expressing shCon or shABRO1 prior to stimulation with control medium (Con), LPS or LPS plus ATP. Cell lysates were immunoblotted with anti-ABRO1 and anti-GAPDH antibodies.

E *Abro1*^{+/+} and *Abro1*^{-/-} BMDMs were left untreated (Con), treated with LPS alone (LPS) or pretreated with LPS, and then stimulated with nigericin, silica, MSU, MDP, Alum, poly(dA:dT), flagellin, or LTx (Anthrax Lethal Factor). CBA analysis of IL-1 β secretion in the culture supernatants.

F Representative immunoblot analysis of cleaved caspase-1 and IL-1 β in culture supernatants (SN) of LPS-primed *Abro1*^{+/+} and *Abro1*^{-/-} BMDMs treated with ATP, nigericin, MSU, flagellin, or poly(dA:dT).

G Flow cytometric analysis of caspase-1 activity in LPS-primed *Abro1*^{+/+} and *Abro1*^{-/-} BMDMs stimulated with nigericin for indicated times.

H Immunostaining of endogenous ASC specks in LPS-primed *Abro1*^{+/+} and *Abro1*^{-/-} BMDMs left untreated or treated with nigericin or poly(dA:dT). Scale bars, 10 μ m.

I Quantification of ASC specks from (H) was performed by counting cells in five random areas of each image in triplicate experiments and described as a percentage of ASC specks for total cell nuclei. At least 100 cells from each treatment condition were quantified. UD, undetectable.

J LPS-primed *Abro1*^{+/+} and *Abro1*^{-/-} BMDMs were left untreated or treated with ATP. Immunoblot analysis of NLRP3 and ASC protein in cell lysates immunoprecipitated with anti-ASC antibody.

Data information: Data are presented as mean \pm SEM from three independent experiments performed in triplicate wells (A–E, G, I) or are representative of three independent experiments (F, H, J). * P < 0.05, ** P < 0.01, *** P < 0.001; ns, not significant; two-tailed unpaired t-test (C–E, I) or two-way ANOVA with Bonferroni post-test (A, B, G).

Source data are available online for this figure.

The maturation and secretion of pro-caspase-1 and pro-IL-1 β are critical steps for inflammasome activation (Franchi *et al*, 2009). We therefore measured the cleavage of pro-IL-1 β and pro-caspase-1. As expected, pro-caspase-1 and pro-IL-1 β were processed to their respective mature forms in LPS-primed *Abro1*^{+/+} BMDMs stimulated with ATP, nigericin, and MSU. However, these effects were significantly inhibited in *Abro1*^{-/-} BMDMs (Fig 1F). In line with these results, significantly reduced active caspase-1 levels were consistently observed in *Abro1*^{-/-} BMDMs compared with *Abro1*^{+/+} BMDMs in response to LPS priming followed by ATP stimulation (Fig 1G). However, flagellin and poly(dA:dT) treatment promoted normal IL-1 β and caspase-1 maturation in *Abro1*^{-/-} BMDMs (Fig 1F), which reconfirmed that ABRO1 was not required for NLRC4 and AIM2 inflammasome activation.

The formation of the adaptor protein ASC speck is another hallmark of inflammasome activation. Once the inflammasome is active, ASC will oligomerize as part of the inflammasome complex to form a single large (up to 2 μ m) perinuclear focus per cell (Fernandes-Alnemri *et al*, 2007). Therefore, we investigated whether ABRO1 deficiency affected ASC speck formation. Compared with *Abro1*^{+/+} BMDMs, the amounts of ASC specks induced by LPS plus nigericin were significantly reduced in *Abro1*^{-/-} BMDMs, whereas ASC speck formation after poly(dA:dT) transfection was unaffected (Fig 1H and I). We also examined the impact of ABRO1 deficiency on ASC oligomerization. The results showed that ASC oligomerization was significantly reduced in *Abro1*^{-/-} BMDMs (Fig EV2B). Moreover, ABRO1 deficiency weakened the interaction between NLRP3 and ASC (Fig 1J). These results provided robust evidence that ABRO1 was necessary for optimal formation of the NLRP3-ASC complex during NLRP3 inflammasome activation.

We also examined whether ABRO1 affected the upstream events of NLRP3 inflammasome activation, including K⁺ efflux, Ca²⁺ mobilization, mitochondrial dysfunction, and ROS generation (He *et al*, 2016). Our results showed that these upstream pathways for NLRP3 activation were unaffected in *Abro1*^{-/-} BMDMs after the respective activator treatment (Fig EV3A–D). It is postulated that ABRO1 acts downstream of K⁺ efflux, Ca²⁺ flux, and mitochondrial damage to control NLRP3 activation.

ABRO1 deficiency attenuated NLRP3-dependent responses *in vivo*

To assess the role of ABRO1 in the regulation of the NLRP3 inflammasome *in vivo*, different NLRP3-dependent inflammatory models were employed. Injection MSU (i.p) into mice can induce NLRP3-dependent IL-1 β production and recruitment of inflammatory cells in the peritoneal cavity (Shenoy *et al*, 2012). As Fig 2A shows, IL-1 β secretion detected in the lavage fluid was significantly decreased in *Abro1*^{-/-} mice (about 60%) and *Nlrp3*^{-/-} mice (about 80%) relative to wild-type mice after MSU injection, but inflammasome-independent TNF- α secretion was unaffected in both knockout mice. Both *Abro1*^{-/-} and *Nlrp3*^{-/-} mice also exhibited impaired recruitment of neutrophils and inflammatory monocytes to the peritoneal cavity compared with wild-type mice (Fig 2B). In addition, caspase-1 activity in recruited *Abro1*^{-/-} immune cells was markedly suppressed (Fig 2C). We also detected significantly lower production of IL-1 β and recruitment of inflammatory cells in the lavage fluid of *Abro1*^{-/-} mice in another NLRP3-dependent peritonitis mouse model induced by Alum (Jin *et al*, 2013; Fig 2D and E). Finally,

ABRO1 deficiency markedly increased mice survival in an LPS-induced sepsis model (Yan *et al*, 2015b; Fig 2F), and *Abro1*^{-/-} animals had a pronounced reduction in serum IL-1 β (Fig 2G), which are consistent with the results in *Nlrp3*^{-/-} mice subjected to a lethal dose of LPS (Mariathasan *et al*, 2006). These results provide evidence that ABRO1 is important for NLRP3 inflammasome activation *in vivo*.

ABRO1 interacts with NLRP3

Based on the current results, ABRO1 is likely to act on the NLRP3 protein itself. Considering that NLRP3 has been identified as a substrate of BRCC3 deubiquitinating enzyme and ABRO1 often performs as an adaptor between BRISC and the substrates (Py *et al*, 2013; Zheng *et al*, 2013), we therefore investigated the association of ABRO1 with subunits of the NLRP3 inflammasome, including NLRP3, ASC, and pro-caspase-1. Co-immunoprecipitation experiment results showed that ABRO1 immunoprecipitated with NLRP3 but not with ASC or pro-caspase-1 (Fig 3A). Detection of an endogenous interaction between ABRO1 and NLRP3 in resting WT BMDMs was difficult; however, the association was substantially increased by LPS priming in a time-dependent manner but was not induced by nigericin or ATP in unprimed cells (Fig 3B and C). In addition, Pam3CSK4, another priming stimulus, also triggered interaction between ABRO1 and NLRP3 (Fig 3D). Interestingly, in LPS-primed macrophages, the interaction between endogenous ABRO1 and NLRP3 almost disappeared after one hour of ATP stimulation or three hours of nigericin stimulation (Fig 3E). These results indicate that ABRO1 engagement by LPS promotes a ternary complex with NLRP3. Mapping of the binding domain targeted by ABRO1 revealed that deletion of either the linker between PYD and NACHT domain (amino acid residues 90–219) or NACHT domain significantly weakened the interaction between NLRP3 and ABRO1; moreover, deletion of both the linker and NACHT domain completely abolished this interaction, indicating that the middle region (amino acid residues 90–536) including the linker between PYD and NACHT domain and NACHT domain is essential for NLRP3 binding to ABRO1 (Fig 3F and G). In addition, the N-terminal region (amino acid residues 1–200) of ABRO1 interacted with NLRP3 (Fig 3H and I).

Phosphorylation of serine 194 in NLRP3 modulates its interaction with ABRO1

Since the interaction of ABRO1 and NLRP3 is augmented upon LPS priming, we assume that post-translational modification is involved in the regulation of ABRO1-NLRP3 complex formation. It has recently been reported that JNK1-mediated NLRP3 phosphorylation at S194 is a critical priming event during NLRP3 inflammasome activation and NLRP3 S194A mutant exhibits a higher level of ubiquitination (Song *et al*, 2017). We therefore investigated whether the phosphorylation status of this residue enabled the recruitment of ABRO1. Constructs of wild-type NLRP3, non-phosphorylated mutant NLRP3 (S194A), or phosphomimetic mutant NLRP3 (S194D; Song *et al*, 2017) were designed and co-transfected into HEK-293T cells with ABRO1. Co-immunoprecipitation assays revealed a robust interaction between NLRP3 (S194D) and ABRO1, but non-phosphorylated NLRP3 mutant S194A significantly weakened this interaction (Fig 4A). Moreover, the interaction between NLRP3 and ABRO1 was augmented in WT

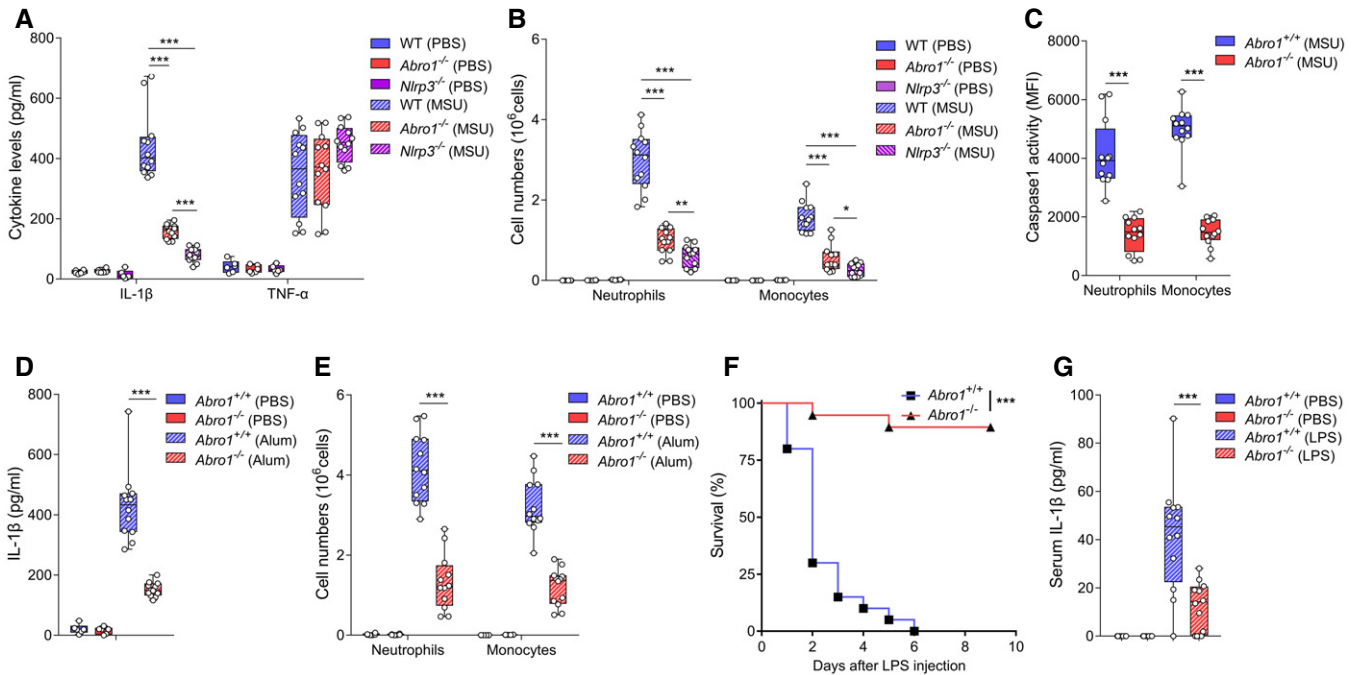


Figure 2. ABRO1 deficiency attenuated NLRP3-dependent responses *in vivo*.

A, B WT, *Abro1*^{-/-}, and *Nlrp3*^{-/-} mice were intraperitoneally injected with MSU (1 mg per mouse) or vehicle (PBS) for 6 h. ELISA of IL-1 β and TNF- α in the peritoneal lavage fluid (A). Flow cytometric analysis of peritoneal cell exudates (B). $n = 6$ for PBS groups and $n = 12$ for MSU groups.
 C *Abro1*^{+/+} and *Abro1*^{-/-} mice were intraperitoneally injected with MSU (1 mg per mouse). Flow cytometric analysis of caspase-1 activity in peritoneal exudate monocytes and neutrophils. $n = 12$ per group.
 D, E *Abro1*^{+/+} and *Abro1*^{-/-} mice were intraperitoneally injected with Alum (1 mg per mouse) or vehicle (PBS) for 6 h. ELISA of IL-1 β in the peritoneal lavage fluid (D) and flow cytometric analysis of peritoneal cell exudates (E). $n = 6$ for PBS groups and $n = 12$ for Alum groups.
 F Survival of *Abro1*^{+/+} and *Abro1*^{-/-} mice subjected to LPS (15 mg/kg). $n = 20$ per group.
 G ELISA of serum IL-1 β from *Abro1*^{+/+} and *Abro1*^{-/-} mice 3 h after intraperitoneal injection of LPS (15 mg/kg) or vehicle (PBS). $n = 6$ for PBS groups and $n = 12$ for LPS groups.

Data information: Data are pooled from two (all PBS groups) or three (C, F, MSU groups of A and B, Alum groups of D–E and LPS groups of G) independent experiments. In (A–E and G), data are shown in box-and-whisker plots: Dots indicate individual mice; box-plot center line, median; box limits, upper and lower quartiles; whiskers show the minimum to maximum. * $P < 0.05$, ** $P < 0.01$, *** $P < 0.001$; log-rank test (F) or two-tailed unpaired t-test (A–E, G).

BMDMs after treatment with the JNK agonist anisomycin (Fig 4B). In contrast, the LPS-induced interaction was significantly reduced by the JNK inhibitor SP600125 (Fig 4C). Consistently, the interaction of the phosphorylation-resistant NLRP3 mutant S194A with ABRO1 is not further enhanced by anisomycin, and that the phosphomimetic NLRP3 mutant S194D is not sensitive to the JNK antagonist SP600125 (Fig 4D and E). These data indicate that JNK1-mediated NLRP3 phosphorylation at S194 is involved in the regulation of the NLRP3 and ABRO1 interaction. To confirm this observation, we characterized the interaction of ABRO1 and NLRP3 in WT and *Nlrp3*^{S194A/S194A} BMDMs by co-immunoprecipitation assays. As shown in Fig 4F, the interaction between ABRO1 and NLRP3 induced by LPS was abolished and not further enhanced by anisomycin in *Nlrp3*^{S194A/S194A} BMDMs compared to that in WT BMDMs. These data support the conclusion that JNK1-mediated NLRP3 phosphorylation at S194 is important for NLRP3 interaction with ABRO1.

ABRO1 promotes the deubiquitination of NLRP3

As deubiquitination by BRCC3 promotes NLRP3 inflammasome activation (Py *et al*, 2013), we examined whether ABRO1 affected

NLRP3 ubiquitination. As shown in Fig 5A, the expression of ubiquitin significantly triggered NLRP3 ubiquitination in HEK-293T cells. However, NLRP3 ubiquitination was diminished by overexpression of ABRO1. We further investigated which poly-ubiquitination pattern of the NLRP3 protein was regulated by ABRO1. The results indicate that overexpression of ABRO1 specifically decreased K63-linked poly-ubiquitination of NLRP3, similar to the reduction in wild-type ubiquitin-linked poly-ubiquitination, but did not affect K48-linked poly-ubiquitination (Fig 5A). Moreover, we mapped the NLRP3 domain targeted by ABRO1, and the data suggest that ABRO1 specifically mediates the deubiquitination of the LRR domain of NLRP3 (Fig 5B). Overexpression of ABRO1 did not affect ASC ubiquitination (Fig EV4A), indicating that ABRO1 is specific for NLRP3 deubiquitination. We also determined whether ABRO1 affected NLRP3 deubiquitination at the endogenous level. The results showed that poly-ubiquitination of endogenous NLRP3 protein was significantly decreased by LPS plus ATP or LPS plus nigericin treatment in *Abro1*^{+/+} BMDMs. However, NLRP3 deubiquitination was not obviously observed in *Abro1*^{-/-} BMDMs in response to this stimulation (Figs 5C and EV4B). Notably, the poly-ubiquitination level of the endogenous NLRP3 protein after LPS priming was comparable in

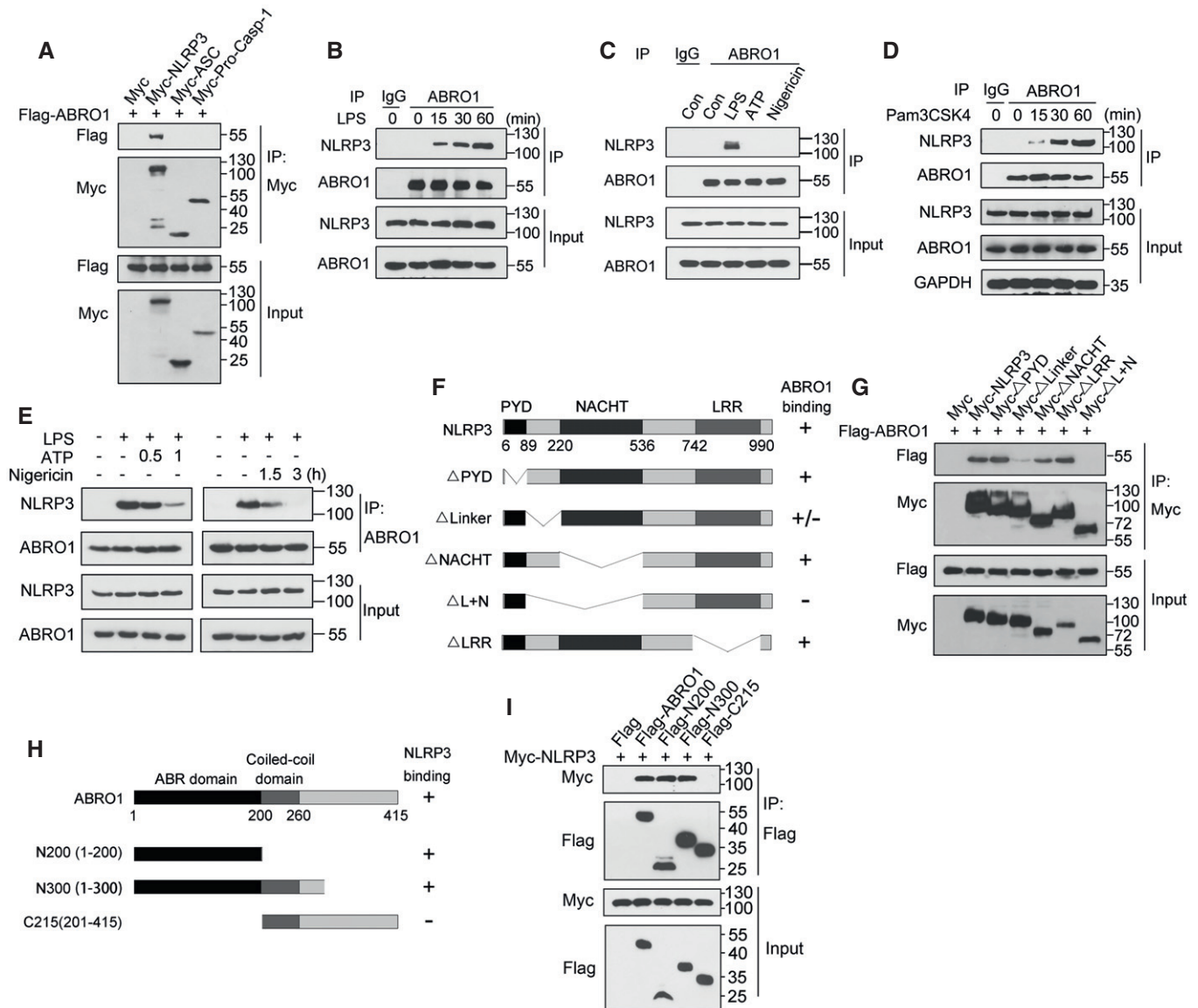


Figure 3. ABRO1 interacts with NLRP3.

A HEK-293T cells were transfected with various combinations (above lanes) of plasmids encoding Flag-ABRO1 and Myc-tagged NLRP3, ASC, or pro-caspase-1 (Pro-Casp-1). Immunoblot analysis of Myc- and Flag-tagged proteins in cell lysates immunoprecipitated with anti-c-Myc agarose.

B–E BMDMs were treated with indicated stimuli. Immunoblot analysis of ABRO1 and NLRP3 proteins in cell lysates immunoprecipitated with control IgG or anti-ABRO1 antibody.

F A schematic representation of NLRP3 wild-type and deletion mutants.

G HEK-293T cells were transfected with various combinations (above lanes) of plasmids encoding Flag-ABRO1 and Myc-tagged NLRP3 or NLRP3 deletion mutants as indicated in (F). Immunoblot analysis of Myc- and Flag-tagged proteins in cell lysates immunoprecipitated with anti-c-Myc agarose.

H A schematic representation of ABRO1 wild-type and deletion mutants.

I HEK-293T cells were transfected with various combinations (above lanes) of plasmids encoding Myc-NLRP3 and Flag-tagged ABRO1 or ABRO1 deletion mutants as indicated in (H). Immunoblot analysis of Myc- and Flag-tagged proteins in cell lysates immunoprecipitated with anti-Flag M2 beads.

Data information: Data are representative of three independent experiments. Source data are available online for this figure.

Abro1^{-/-} and WT BMDMs (Figs 5C and EV4B). Taken together, these data indicate that ABRO1 mediates K63-linked deubiquitination of NLRP3 induced by the activation signals.

The NLRP3 auto-activating mutations are involved in auto-inflammatory diseases (Masters *et al*, 2009), and these mutations

can be directly activated by LPS alone (Gattorno *et al*, 2007). Our results found that LPS induced significant deubiquitination of NLRP3 (A350V) mutant which is responsible for Muckle–Wells syndrome (MWS), a kind of cryopyrin-associated periodic syndrome (CAPS), where ATP was unable to induce further

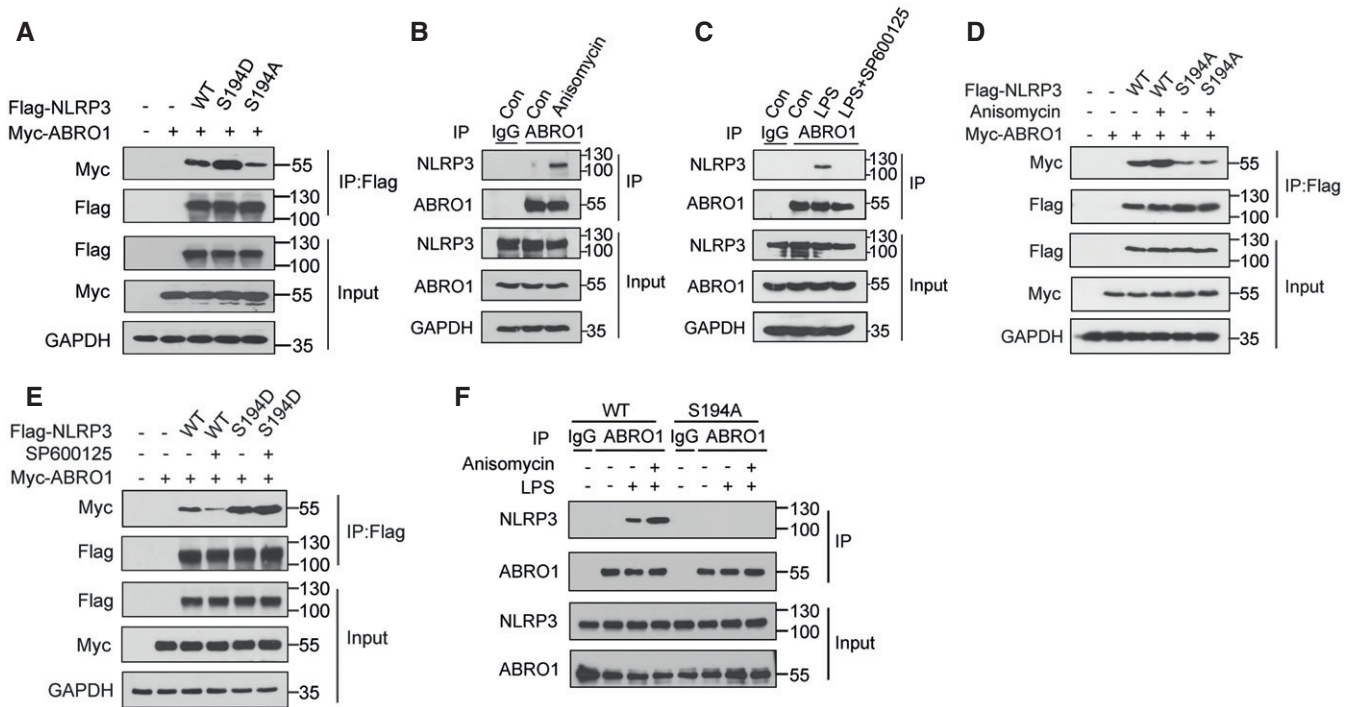


Figure 4. Phosphorylation of serine 194 in NLRP3 modulates the interaction with ABRO1.

A HEK-293T cells were transfected with various combinations (above lanes) of plasmids encoding Myc-ABRO1 and Flag-tagged NLRP3 (WT), NLRP3 (S194D), or NLRP3 (S194A). Immunoblot analysis of Myc- and Flag-tagged proteins in cell lysates immunoprecipitated with anti-Flag M2 beads.

B WT BMDMs were treated with or without 5 μ M Anisomycin for 2 h. Immunoblot analysis of NLRP3 and ABRO1 proteins in cell lysates immunoprecipitated with control IgG or anti-ABRO1 antibody.

C WT BMDMs were pretreated with or without 100 nM SP600125 for 1 h and then left untreated or treated with 100 ng/ml LPS for 1 h. Immunoblot analysis of NLRP3 and ABRO1 proteins in cell lysates immunoprecipitated with control IgG or anti-ABRO1 antibody.

D HEK-293T cells transfected with various combinations (above lanes) of plasmids encoding Myc-ABRO1 and Flag-NLRP3 (WT) or Flag-NLRP3 (S194A) were treated with or without 5 μ M Anisomycin for 2 h. Immunoblot analysis of Myc- and Flag-tagged proteins in cell lysates immunoprecipitated with anti-Flag M2 beads.

E HEK-293T cells transfected with various combinations (above lanes) of plasmids encoding Myc-ABRO1 and Flag-NLRP3 (WT) or Flag-NLRP3 (S194A) were treated with or without 100 nM SP600125 for 2 h. Immunoblot analysis of Myc- and Flag-tagged proteins in cell lysates immunoprecipitated with anti-Flag M2 beads.

F WT and *Nlrp3*^{S194A/S194A} BMDMs were pretreated with or without 5 μ M Anisomycin for 2 h and then left untreated or treated with 100 ng/ml LPS for 1 h. Immunoblot analysis of NLRP3 and ABRO1 proteins in cell lysates immunoprecipitated with control IgG or anti-ABRO1 antibody.

Data information: Data are representative of three independent experiments.
Source data are available online for this figure.

deubiquitination (Figs 5D and EV4C). After plasmids encoding HA-tagged ubiquitin (HA-Ub) and Flag-NLRP3 (A350V) were transiently transfected into HEK-293T cells with or without ABRO1, the NLRP3 (A350V) ubiquitination triggered by the expression of ubiquitin was significantly diminished by the overexpression of ABRO1 (Fig 5E). In addition, LPS also promoted the interaction of ABRO1 and NLRP3 (A350V; Fig 5F). These results indicate that ABRO1 is also involved in deubiquitination of NLRP3 auto-activating mutations.

Furthermore, treatment with the JNK agonist anisomycin promoted ABRO1-mediated NLRP3 deubiquitination, while JNK inhibitor SP600125 treatment reduced ABRO1-mediated NLRP3 deubiquitination (Fig 5G). Consistent with these results, deubiquitination of NLRP3 induced by LPS plus ATP treatment was significantly inhibited in *Nlrp3*^{S194A/S194A} BMDMs (Fig 5H). These data suggest that JNK-mediated S194 phosphorylation on NLRP3 positively regulates NLRP3 deubiquitination induced by activator stimulation.

ABRO1 facilitates NLRP3 deubiquitination dependent on BRCC3

Since ABRO1 is an important subunit of BRISC, we hypothesized that ABRO1 synergized with BRCC3 to promote NLRP3 inflammasome activation. We generated *Brcc3*-deficient mice to explore this hypothesis (Fig EV5A and B). *Brcc3*^{-/-} mice were viable, fertile, and exhibited normal development and life spans. Immunoprecipitation assays performed in LPS-primed BMDMs showed that both BRCC3 and ABRO1 co-precipitated with NLRP3 using anti-NLRP3 antibodies. Similar results were observed when immunoprecipitation assays were performed with BRCC3- and ABRO1-specific antibodies (Fig 6A), suggesting that these three proteins may form a complex during the priming step of NLRP3 inflammasome activation. Furthermore, NLRP3 co-precipitated with ABRO1 in LPS-primed *Brcc3*^{-/-} BMDMs (Fig 6B), indicating that BRCC3 is dispensable for the interaction between ABRO1 and NLRP3. In contrast, NLRP3 could not co-precipitate with BRCC3 in LPS-primed *Abro1*^{-/-} BMDMs, which was not associated with changes in

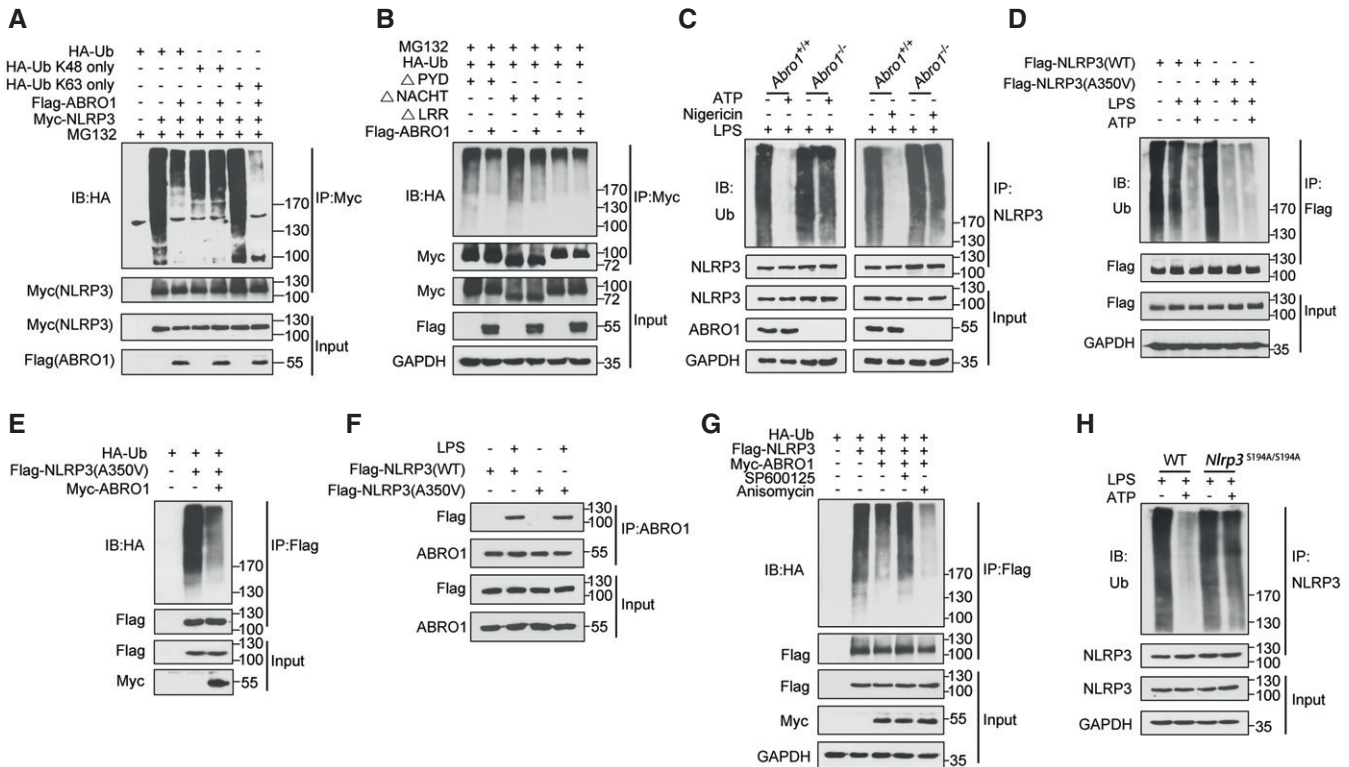


Figure 5. ABRO1 promotes deubiquitination of NLRP3.

- A** HEK-293T cells were transfected with various combinations (above lanes) of plasmids encoding Myc-NLRP3, Flag-ABRO1 and HA-ubiquitin (HA-Ub), HA-Ub K48 only, or K63 only. Before collection, cells were treated with MG132 (10 μ M) for 6 h. Immunoblot analysis of NLRP3 ubiquitination (detected by anti-HA antibody) in cell lysates immunoprecipitated with anti-c-Myc agarose.
- B** HEK-293T cells were transfected with various combinations (above lanes) of plasmids encoding HA-Ub, Flag-ABRO1, and NLRP3 truncations as indicated. Before collection, cells were treated with MG132 (10 μ M) for 6 h. Immunoblot analysis of ubiquitination of NLRP3 truncations (detected by anti-HA antibody) in cell lysates immunoprecipitated with anti-c-Myc agarose.
- C** LPS-primed *Abro1*^{+/+} and *Abro1*^{-/-} BMDMs were left untreated or treated with ATP (left) or nigericin (right). Immunoblot analysis of NLRP3 ubiquitination (detected by mouse anti-ubiquitin antibody) in cell lysates immunoprecipitated with rabbit anti-NLRP3 antibody.
- D** *Nlrp3*^{-/-} BMDMs transduced with lentiviruses expressing Flag-NLRP3 (WT) or Flag-NLRP3 (A350V) were left unstimulated or stimulated with LPS or LPS plus ATP. Immunoblot analysis of NLRP3 and NLRP3 (A350V) ubiquitination (detected by mouse anti-ubiquitin antibody) in cell lysates immunoprecipitated with anti-Flag M2 beads.
- E** HEK-293T cells were transfected with various combinations (above lanes) of plasmids encoding Myc-ABRO1, Flag-NLRP3 (A350V), and HA-ubiquitin (HA-Ub). Immunoblot analysis of NLRP3 (A350V) ubiquitination (detected by anti-HA antibody) in cell lysates immunoprecipitated with anti-Flag M2 beads.
- F** *Nlrp3*^{-/-} BMDMs transduced with lentiviruses expressing Flag-NLRP3 (WT) or Flag-NLRP3 (A350V) were stimulated with or without 100 ng/ml LPS for 1 h. Immunoblot analysis of ABRO1 and NLRP3 proteins in cell lysates immunoprecipitated with anti-ABRO1 antibody.
- G** HEK-293T cells transfected with various combinations (above lanes) of plasmids encoding Myc-ABRO1, Flag-NLRP3, and HA-ubiquitin (HA-Ub) were left untreated or treated with 5 μ M Anisomycin for 2 h or 100 nM SP600125 for 2 h. Immunoblot analysis of NLRP3 ubiquitination (detected by anti-HA antibody) in cell lysates immunoprecipitated with anti-Flag M2 beads.
- H** LPS-primed WT and *Nlrp3*^{S194A/S194A} BMDMs were left untreated or treated with ATP. Immunoblot analysis of NLRP3 ubiquitination (detected by mouse anti-ubiquitin antibody) in cell lysates immunoprecipitated with rabbit anti-NLRP3 antibody.

Data information: Data are representative of three independent experiments.

Source data are available online for this figure.

NLRP3 or BRCC3 levels in *Abro1*^{-/-} BMDMs (Fig 6C). In addition, overexpression of ABRO1 promoted the interaction between BRCC3 and NLRP3 (Fig 6D). These data suggest that ABRO1 is an essential scaffold for the interaction of NLRP3 with BRCC3. Consistent with these interaction findings, overexpression of BRCC3 significantly increased deubiquitination of NLRP3 induced by LPS plus nigericin stimuli in *Brc3*^{-/-} BMDMs (Fig 6E), whereas overexpression of BRCC3 in *Abro1*^{-/-} BMDMs could not rescue NLRP3 deubiquitination (Fig 6F). Similar results were obtained upon overexpression of

ABRO1 in *Abro1*^{-/-} and *Brc3*^{-/-} BMDMs (Fig 6E and F). These data suggest that BRCC3 facilitates NLRP3 deubiquitination in an ABRO1-dependent manner. In WT BMDMs, overexpression of ABRO1 or BRCC3 significantly promoted the secretion of IL-1 β after LPS plus ATP treatment (Fig 6G and H). In *Brc3*^{-/-} BMDMs, reverse transfection of BRCC3 significantly rescued the decrease in IL-1 β production. However, the decrease in IL-1 β production could not be rescued by transfection of ABRO1 in *Brc3*^{-/-} BMDMs (Fig 6G). Similarly, the decrease in IL-1 β production in

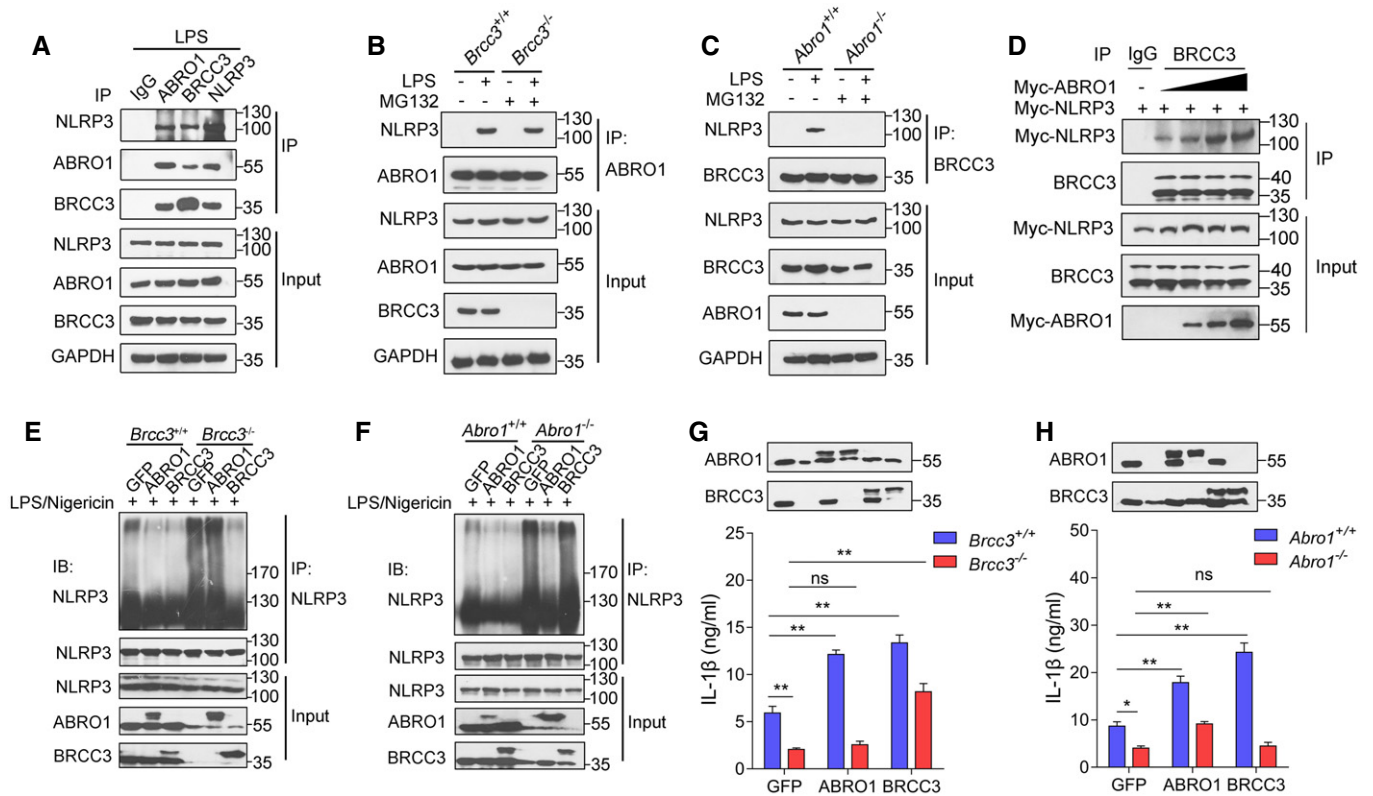


Figure 6. ABRO1 facilitates NLRP3 deubiquitination dependent on BRCC3.

A WT BMDMs were stimulated with LPS for 1 h. Immunoblot analysis of NLRP3, ABRO1, and BRCC3 from the cell lysates immunoprecipitated with control IgG, anti-ABRO1, anti-BRCC3, or anti-NLRP3 antibody.

B *Brc3^{+/+}* and *Brc3^{-/-}* BMDMs were treated with or without LPS for 1 h. Before LPS treatment, *Brc3^{-/-}* BMDMs were pretreated with MG132 (10 μ M) for 6 h to rescue the expression of ABRO1. Immunoblot analysis of NLRP3 and ABRO1 proteins in cell lysates immunoprecipitated with anti-ABRO1 antibody.

C *Abro1^{+/+}* and *Abro1^{-/-}* BMDMs were treated with or without LPS for 1 h. Before LPS treatment, *Abro1^{-/-}* BMDMs were pretreated with MG132 (10 μ M) for 6 h to rescue the expression of BRCC3. Immunoblot analysis of NLRP3 and BRCC3 proteins in cell lysates immunoprecipitated with anti-BRCC3 antibody.

D A constant amount of Myc-NLRP3 plasmid together with an increasing amount of Myc-ABRO1 plasmid was co-transfected in HEK-293T cells. Immunoblot analysis of NLRP3 and BRCC3 from the cell lysates immunoprecipitated with control IgG or anti-BRCC3 antibody.

E–H *Abro1^{+/+}*, *Abro1^{-/-}*, *Brc3^{+/+}*, and *Brc3^{-/-}* BMDMs transduced with lentiviruses expressing GFP, ABRO1-GFP, or BRCC3-GFP were treated with LPS and nigericin. Immunoblot analysis of NLRP3 ubiquitination (detected by mouse anti-NLRP3 antibody) in cell lysates immunoprecipitated with rabbit anti-NLRP3 antibody (E, F). CBA analysis of IL-1 β in culture supernatants (G, H).

Data information: Data are presented as mean \pm SEM from three independent experiments performed in triplicate wells (G and H) or are representative of three independent experiments (A–F). * $P < 0.05$, ** $P < 0.01$; ns, not significant; two-tailed unpaired t-test (G and H). Source data are available online for this figure.

Abro1^{-/-} BMDMs was significantly rescued by reverse transfection of ABRO1 but not by transfection of BRCC3 (Fig 6H). It is concluded that ABRO1 synergizes with BRCC3 to promote NLRP3 inflammasome activation by regulating NLRP3 deubiquitination.

BRCC3 mediates activation of the NLRP3 inflammasome *in vitro* and *in vivo*

Next, we investigated the role of BRCC3 in the activation of NLRP3 inflammasome. Stimulation with ATP, nigericin, MSU, and Alum induced pronounced secretion of mature IL-1 β in LPS-primed BMDMs from WT mice, but this response was considerably reduced in cells from *Brc3^{-/-}* mice (Fig 7A). However, IL-1 β secretion stimulated by poly(dA:dT) and flagellin was not influenced in *Brc3^{-/-}* BMDMs (Fig 7A). Importantly, BRCC3 deficiency had no inhibitory

effects on IL-6 and TNF- α secretion or *Il1b* mRNA expression after LPS stimulation (Fig EV5C and D). In addition, BRCC3 deficiency significantly inhibited the cleavage of pro-IL-1 β and pro-caspase-1 in response to nigericin, ATP, or MSU stimulation but not to poly(dA:dT) and flagellin treatment (Fig 7B), and the formation of ASC speck induced by nigericin was significantly inhibited but remained unperturbed when induced by poly(dA:dT) in *Brc3^{-/-}* BMDMs (Figs 7C and EV5E). These results indicate that BRCC3 deficiency specifically inhibits the activation of the NLRP3 inflammasome. Consistent with that in *Abro1^{-/-}* BMDMs, NLRP3 deubiquitination induced by LPS plus nigericin treatment was significantly inhibited in *Brc3^{-/-}* BMDMs; however, comparable levels of poly-ubiquitination of the endogenous NLRP3 protein after LPS priming were observed in *Brc3^{-/-}* and WT BMDMs (Figs 7D and EV5F).

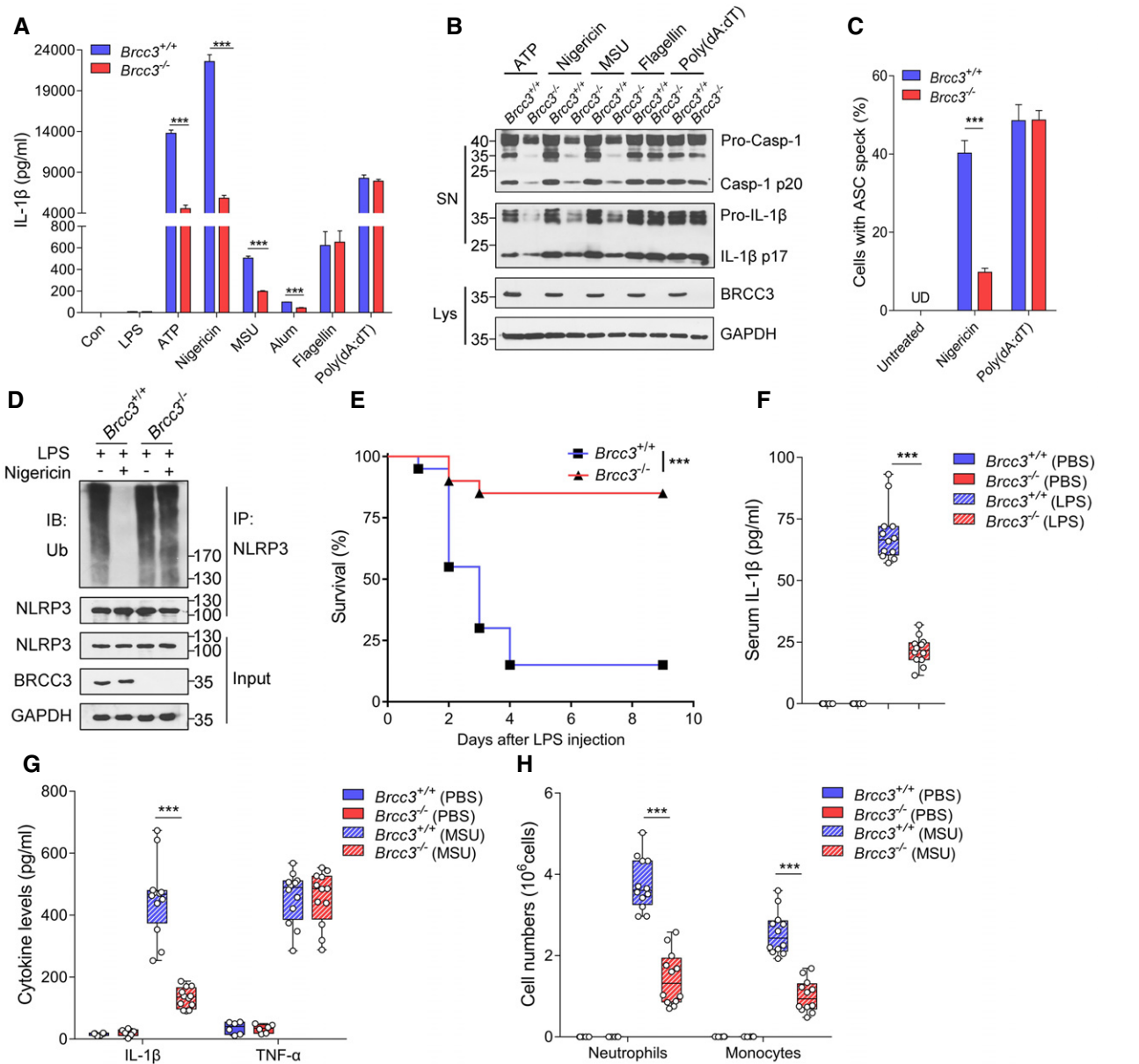


Figure 7. BRCC3 mediates activation of the NLRP3 inflammasome *in vitro* and *in vivo*.

A *Brcc3*^{+/+} and *Brcc3*^{-/-} BMDMs were left untreated (Con), treated with LPS alone (LPS) or pretreated with LPS, and then stimulated with ATP, nigericin, MSU, Alum, poly (dA:dT), or flagellin. CBA analysis of IL-1β secretion in the culture supernatants.

B Immunoblot analysis of cleaved caspase-1 and IL-1β in culture supernatants (SN) of LPS-primed *Brcc3*^{+/+} and *Brcc3*^{-/-} BMDMs treated with ATP, nigericin, MSU, flagellin, and poly (dA:dT).

C Immunostaining of endogenous ASC specks in LPS-primed *Brcc3*^{+/+} and *Brcc3*^{-/-} BMDMs left untreated or treated with nigericin or poly(dA:dT). ASC speck positive cells were counted and analyzed as described in Fig 11. UD, undetectable.

D LPS-primed *Brcc3*^{+/+} and *Brcc3*^{-/-} BMDMs were left unstimulated or stimulated with nigericin. Immunoblot analysis of NLRP3 ubiquitination (detected by mouse anti-ubiquitin antibody) in cell lysates immunoprecipitated with rabbit anti-NLRP3 antibody.

E Survival of *Brcc3*^{+/+} and *Brcc3*^{-/-} mice subjected to LPS (15 mg/kg). *n* = 20 per group.

F ELISA of serum IL-1β from *Brcc3*^{+/+} and *Brcc3*^{-/-} mice 3 h after intraperitoneal injection of LPS (15 mg/kg) or vehicle (PBS). *n* = 6 for PBS groups and *n* = 12 for LPS groups.

G, H *Brcc3*^{+/+} and *Brcc3*^{-/-} mice were intraperitoneally injected with MSU (1 mg per mouse) or vehicle (PBS) for 6 h. ELISA of IL-1β and TNF-α in the peritoneal lavage fluid (G) and flow cytometric analysis of peritoneal cell exudates (H). *n* = 6 for PBS groups and *n* = 12 for MSU groups.

Data information: Data are presented as mean ± SEM from three independent experiments performed in triplicate wells (A and C) or are representative of three independent experiments (B and D). In (E–H), data are pooled from two (all PBS groups) or three (E, LPS groups of F, MSU groups of G–H) independent experiments. In (F–H), data are shown in box-and-whisker plots: Dots indicate individual mice; box-plot center line, median; box limits, upper, and lower quartiles; whiskers show the minimum to maximum. ****P* < 0.001; log-rank test (E) or two-tailed unpaired *t*-test (A, C, F–H).

Source data are available online for this figure.

To further explore the physiological role of BRCC3 in NLRP3 inflammasome activation, we next investigated the effects of BRCC3 in a mouse model of LPS-induced endotoxemia. Similar to deletion of ABRO1 or NLRP3 (Mariathasan *et al*, 2006), BRCC3 deficiency markedly increased mice survival after injection of a lethal dose of LPS (Fig 7E) and resulted in a pronounced reduction in serum IL-1 β (Fig 7F). These data are consistent with our earlier findings that indicate a role for BRCC3 in controlling IL-1 β maturation *in vitro*. Moreover, in MSU-induced peritonitis, a significant reduction of NLRP3-dependent IL-1 β production and inflammatory cell recruitment in the peritoneal cavity were observed in *Brc3*^{-/-} mice compared with WT mice (Fig 7G and H). Overall, these results suggest that BRCC3 deficiency displays similar phenotypes of ABRO1 knockout mice.

Discussion

In this paper, we describe an ABRO1-mediated regulatory signaling system that controls the activation of the NLRP3 inflammasome. Our results showed that ABRO1 deficiency resulted in remarkable attenuation of recruitment of ASC to NLRP3, formation of ASC specks, activation of caspase-1, and release of IL-1 β and IL-18 in BMDMs upon treatment with NLRP3 ligands after the priming step. Moreover, these results were confirmed in BMDMs lacking BRCC3, the catalytically active component of BRISC. These data indicate that NLRP3 inflammasome activation is controlled by BRISC. The discrepancy between our results and those reported by Zheng *et al* (2013) may be due to the fact that they have not detected the cleaved caspase-1 and IL-1 β released from cells, and the samples from their ABRO1 knockout cells are overexposed compared to the wild-type cells. Importantly, our present study demonstrates that, in more physiological settings, mice lacking either ABRO1 or BRCC3 exhibit severely reduced inflammation in response to NLRP3 inflammasome activation in *in vivo* animal models, as shown by reduced IL-1 β secretion and attenuated recruitment of immune cells. Therefore, our results extend previous work by showing a role of BRCC3 in the regulation of NLRP3 inflammasome activation in more detail and provide clear genetic evidence from knockout mice.

Two sequential steps of deubiquitination of NLRP3 are reported to be involved in NLRP3 inflammasome activation (Juliana *et al*, 2012; Palazon-Riquelme *et al*, 2018). LPS priming induces the first step deubiquitination of NLRP3 and up-regulates steady-state NLRP3 protein levels (Han *et al*, 2015). Activation step causes an additional decrease in ubiquitinated NLRP3, which almost completely removes all types of ubiquitin chains from NLRP3 (Juliana *et al*, 2012). Given the previously described role of BRCC3 in NLRP3 deubiquitination and that ABRO1 is an important subunit of BRCC3 complex, we assume that ABRO1 may be involved in the regulation of NLRP3 deubiquitination. Indeed, we found that activation signal-induced NLRP3 deubiquitination was significantly suppressed in *Abro1*^{-/-} and *Brc3*^{-/-} BMDMs, indicating that BRISC is a critical regulator of NLRP3 inflammasome through deubiquitination of NLRP3. Previous publications have reported that high concentrations of DUB inhibitors, such as G5, ESI, WP1130, and b-AP15, almost completely suppress the release of IL-1 β in response to NLRP3 inflammasome activation (Lopez-Castejon *et al*, 2013; Py *et al*, 2013). We note that

IL-1 β release was generally only reduced by about 70% in *Abro1*^{-/-} and *Brc3*^{-/-} BMDMs relative to wild-type cells after LPS plus ATP or LPS plus nigericin treatment. However, the IL-1 β release was almost completely blocked in *Nlrp3*^{-/-} BMDMs. Moreover, ABRO1 deficiency resulted in remarkable but not complete attenuation of IL-1 β secretion and immune cells recruitment in MSU-induced peritonitis model. These data indicate that BRISC is not absolutely required for NLRP3 activation, and other DUBs may also be involved in the regulation of NLRP3 deubiquitination.

Data from several publications suggest that phosphorylation and poly-ubiquitination of NLRP3 may be linked phenomena that operate in tandem to regulate NLRP3 activation (Guo *et al*, 2016; Song *et al*, 2017). However, the potential mechanism is unknown. NLRP3 S194A mutant has been observed to exhibit a higher level of ubiquitination (Song *et al*, 2017), suggesting that JNK1-mediated NLRP3 phosphorylation at S194 may be involved in the regulation of NLRP3 ubiquitination. We found that LPS priming induced ABRO1 binding to NLRP3 in an S194 phosphorylation-dependent manner, and inhibition of NLRP3 S194 phosphorylation by JNK inhibitor SP600125 or non-phosphorylated mutant NLRP3 (S194A) almost completely blocked the interaction between ABRO1 and NLRP3, consequently suppressing ABRO1-mediated NLRP3 deubiquitination. Thus, in addition to activating NF- κ B-mediated NLRP3 transcription, the LPS priming signal also rapidly induces NLRP3 S194 phosphorylation (Song *et al*, 2017) and promotes ABRO1 binding to NLRP3. Subsequently, ABRO1 acts as a scaffold to assemble the BRISC which mediates deubiquitination of NLRP3 upon the stimulation with activation signals, followed by recruitment of ASC to NLRP3, formation of ASC specks, activation of caspase-1, and release of mature IL-1 β . Although LPS stimulation induces an interaction between ABRO1 and NLRP3, deficiency in either ABRO1 or BRCC3 suppresses NLRP3 deubiquitination only in response to LPS priming plus ATP or nigericin stimulation, but not to LPS priming alone, indicating that driving BRISC to deubiquitinate NLRP3 requires both the priming and the activation signal. NLRP3 is auto-repressed owing to an internal interaction between the NACHT domain and LRRs under normal cellular conditions (Tschopp & Schroder, 2010). According to the present and previous studies, BRISC specifically mediates the deubiquitination of the LRR domain of NLRP3 (Py *et al*, 2013). The auto-repressed state of NLRP3 therefore may keep BRISC from targeting to NLRP3, enabling the cells to maintain a high level of poly-ubiquitinated NLRP3, even in presence of priming signals alone. Upon stimulation with activators, NLRP3 can undergo a conformational change, leading to the exposure of the NACHT domain and LRRs (Kanneganti & Lamkanfi, 2013), thereby promoting BRISC-mediated NLRP3 deubiquitination. In this way, BRISC could rapidly deubiquitinate and activate NLRP3 (Fig 8). Supporting this contention, NLRP3 (A350V) mutation, which is believed to be in a conformational state that removes the necessity for an activation agonist to drive its activation (Kanneganti & Lamkanfi, 2013), underwent BRISC-dependent deubiquitination induced by LPS alone. This model provides new insights into the molecular mechanism for the regulation of NLRP3 activation and the implications for the treatment of NLRP3 inflammasome-related diseases.

In our present study, ATP induces almost thorough deubiquitination of NLRP3 in WT cells but only mild deubiquitination in ABRO1 and BRCC3 knockout cells after LPS priming. These results indicate

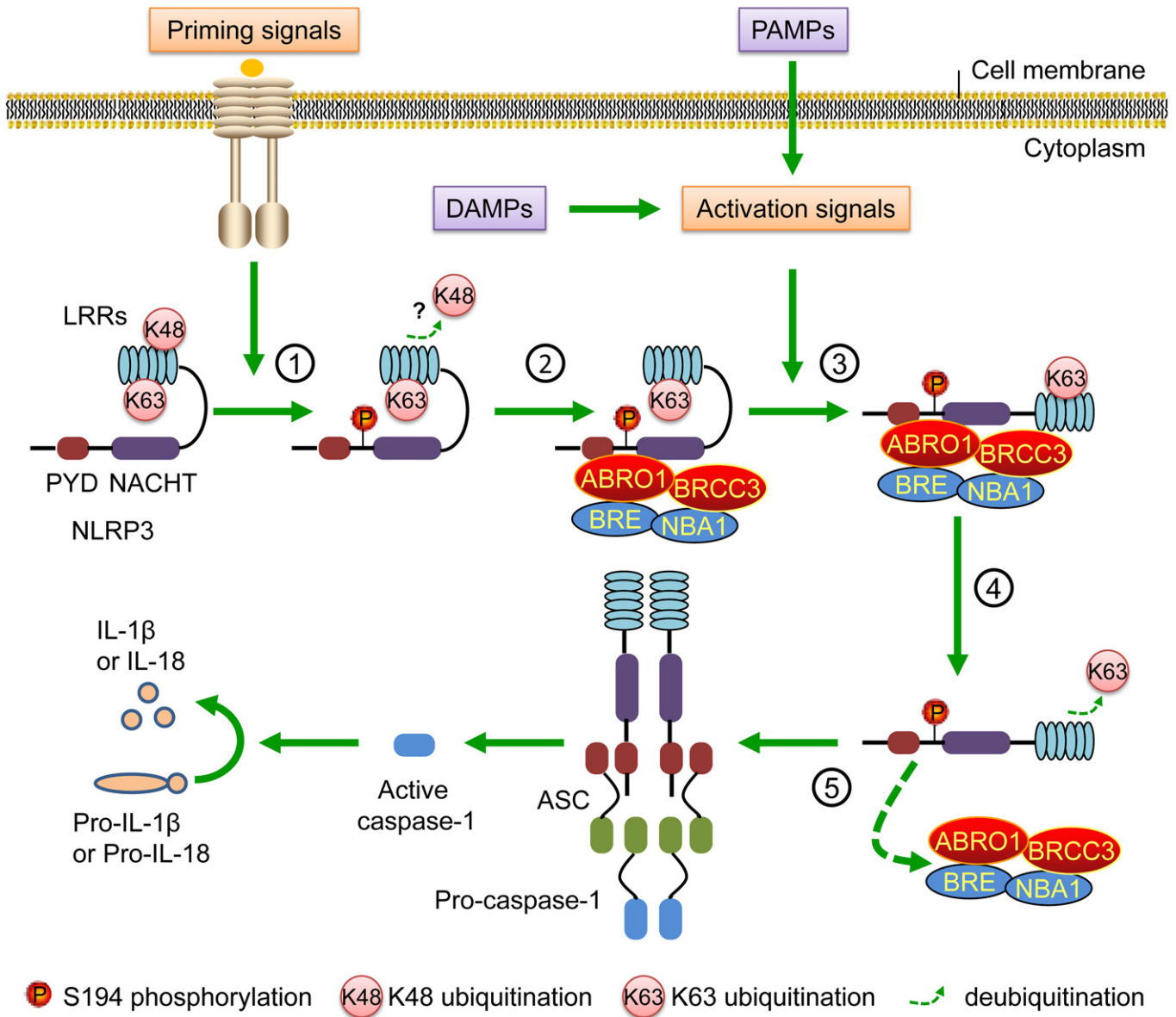


Figure 8. Schematic diagram of the mechanism of NLRP3 inflammasome activation regulated by ABRO1.

In resting macrophages, NLRP3 is poly-ubiquitinated with mixed Lys-48 and Lys-63 ubiquitin chains. NLRP3 is auto-repressed owing to an internal interaction between the NACHT domain and LRRs. Priming signals induce S194 phosphorylation and the first step of deubiquitination of NLRP3 (1). ABRO1 binds to S194 phosphorylated NLRP3, subsequently recruiting the BRISC complex to NLRP3 (2). In the presence of activation signals, NLRP3 undergoes a conformational change, resulting in exposure of the LRR domain (3). BRISC complex removes K63-linked ubiquitin chains of LRR domain, leading to the activation of NLRP3 (4). Then, BRISC complex dissociates from NLRP3. In turn, the activated NLRP3 recruits ASC and pro-caspase-1 to assemble the inflammasome complex (5), triggering the activation of caspase-1 followed by the processing and secretion of pro-inflammatory cytokines such as IL-1 β and IL-18.

that the K63-linked polyubiquitin chains remained on NLRP3 after LPS priming. However, what proportion of the NLRP3 is poly-ubiquitinated that is still undetermined. This may be due to the lack of a defined antibody which can equally well recognize all forms of NLRP3 protein. The model proposed here suggests that a majority of NLRP3 is poly-ubiquitinated and the ubiquitin needs to be removed to allow oligomerization. However, we cannot exclude the possibility that only some fraction of NLRP3 is ubiquitinated after LPS priming. Considering

that NLRP3 must multimerize to assemble the inflammasome complex (Cai *et al*, 2014), having just a small fraction of ubiquitinated NLRP3 may be sufficient to prevent the complex being functional. Alternatively, there may be a more complex mechanism that we do not yet fully understand.

Abnormally elevated NLRP3 inflammasome signaling has been linked with various human autoinflammatory and autoimmune diseases (Menu & Vince, 2011). Recently, a few NLRP3 specific inhibitors, such as MCC950 and Cy-09, have been developed and tested

in animal models (Coll *et al.*, 2015; Jiang *et al.*, 2017). However, there is still a lack of drugs that directly interfere with NLRP3 inflammatory activation in clinical treatment. Data presented here showed that inactivation of BRISC significantly reduced the severity of NLRP3-associated inflammatory diseases in animals. Importantly, various DUBs are emerging as attractive therapeutic targets in diseases ranging from oncology to neurodegeneration, and first-generation DUB inhibitors are now approaching clinical trials (Harrigan *et al.*, 2018). Thus, the identification of selective inhibitors or antagonists of DUB activity of BRISC may represent a novel and promising strategy to treat NLRP3 inflammasome-associated diseases. Furthermore, according to our study, it is ABRO1 that mediates the interaction of NLRP3 with BRCC3. ABRO1 binds to the middle region (amino acid residues 90–536) of NLRP3 including NACHT domain and the linker between PYD and NACHT domain. Besides, the interaction is dependent on the phosphorylation of NLRP3 at S194. Therefore, targeting ABRO1-NLRP3 interaction may be an alternative drug discovery strategy for NLRP3 inflammasome-associated diseases. In addition, in LPS-primed macrophages, the interaction between endogenous ABRO1 and NLRP3 disappeared upon nigericin or ATP stimulation, implying that this key molecular mechanism of NLRP3 deubiquitination mediated by ABRO1 may contribute to the self-limiting regulation of inflammasome activation (Kim *et al.*, 2016). Further studies are required to clarify the contribution of the ABRO1-mediated NLRP3 deubiquitination regulatory signaling system to human NLRP3 inflammasome-associated diseases.

In summary, our data represent the first evidence that ABRO1 plays a key role in regulating NLRP3 inflammasome activation *in vitro* and *in vivo*. The mechanisms of NLRP3-associated ABRO1 action provide new insights on identifying other BRISC-targeted substrates. Targeting ABRO1-NLRP3 interaction or BRISC DUB activity may represent new therapeutic strategies in fighting NLRP3-associated inflammatory diseases.

Materials and Methods

Mice

Abro1^{-/-} mice were generated by the Model Animal Research Center of Nanjing University using classical gene targeting by homologous recombination in C57BL/6J ES cells. *Brcc3*^{-/-} mice were generated by BIOCYTOGEN using CRISPR/Cas9-mediated genome editing on a C57/BL/6J background. *Nlrp3*^{-/-} mice were a generous gift from Tao Li (National Center of Biomedical Analysis, Beijing, China). All these mouse strains were maintained in specific pathogen-free conditions at the Animal Facility of our institute. All animal experiments were reviewed and approved by the Institutional Animal Care and Use Committee of our institution. Male and female mice between 6 and 10 weeks of age were used in the studies.

Cell culture

Bone marrow-derived macrophages (BMDMs) were obtained from C57BL/6J or mutant mice as described (Zhang *et al.*, 2008). Briefly, BMDMs were isolated from bone marrow of 8-week-old mice and

cultured in RPMI-1640 medium complemented with 10% heated inactivated FBS (Gibco, 10270), 1% penicillin/streptomycin (P/S), and 20–30% L929 culture supernatant for 7 days. L929 cells were cultured in RPMI-1640 medium complemented with 10% FBS, 1% (P/S). HEK-293T cells were cultured in Dulbecco's modified Eagle's medium (DMEM) supplemented with 10% FBS and 1% P/S. Cells were incubated in a humidified chamber with 5% CO₂ at 37°C for growth.

Primary human mononuclear cells were isolated from umbilical cord blood in healthy donors using Ficoll-Paque. Human CD14⁺ monocytes were sorted from mononuclear cells by using Human Monocyte Isolation Kit II (Miltenyi, 130-091-153) according to the manufacturer's instructions. Human umbilical cord blood units were collected from normal, microbiologically screened and ethics-cleared donors with informed consent of the mothers. The participants have provided their written informed consent. All investigations were approved by the Institutional Research Ethics Committee of our institution. Human monocyte-derived macrophages (HMDMs) were generated from CD14⁺ monocytes by differentiation for 7 days in RPMI-1640 supplemented with 10% FBS, 1% P/S, and 30 ng/ml human M-CSF (Peprotech, 300-25). Human data experiments conformed to the principles set out in the WMA Declaration of Helsinki and the Department of Health and Human Services Belmont Report.

Plasmids and transfection

Flag-mouse NLRP3 (WT, S194A, and S194D), and Flag-human NLRP3 plasmids were a kind gift of Dr. Tao Li (National Center of Biomedical Analysis, Beijing, China). Myc-human NLRP3, Myc-human ASC, and Myc-human pro-caspase-1 plasmids were kindly provided by Dr. Jian Wang (Beijing Proteome Research Center, China). HA-ubiquitin, HA-ubiquitin K48-only (all lysines mutated to arginine except K48; forms only K48-linked chains), and HA-ubiquitin K63-only (all lysines mutated to arginine except K63; forms only K63-linked chains) plasmids were a generous gift from Dr. Xueming Zhang (National Center of Biomedical Analysis, Beijing, China). Deletion mutants of human NLRP3 and the full length of human ABRO1 were cloned into the pcDNA3.1/myc-His-B plasmid (Invitrogen). Full length and deletion mutants of human ABRO1 were constructed using pFlag-CMV-2 (Sigma). Retroviral expression constructs for mouse ABRO1, mouse BRCC3, mouse NLRP3, and mouse NLRP3 (A350V) were cloned into the pCDH-MCS-T2A-copGFP-MSCV expression vector (pCDH-GFP; System Biosciences, CD523A-1). Human ABRO1 shRNAs (shABRO1: 5-CAGAGGATATCACTCGCTATT-3) and scramble shRNAs (shCon: 5-CCTAAGGTTAAGTCGCCCTCG-3) were cloned into the pLKO.1-GFP vector (Addgene). Transient transfections were performed using Lipofectamine 2000 Transfection Reagent (Invitrogen, 11668019), according to the manufacturer's instructions, in HEK-293T cells.

Lentivirus production and infection

To prepare the lentivirus particles, HEK-293T cells in the 10-cm dish were transfected with 15 µg of expression vectors together with 15 µg of psPAX2 (Addgene) and 5 µg of pMD2.G (Addgene). Eight hours after transfection, the media were changed to DMEM supplemented with 10% FBS and 1% P/S. Another 40 h later, the media

were collected and centrifuged at 900 g for 10 min. The supernatant was filtered through a 0.45- μ m membrane. Cold PEG-*it* Virus Precipitation Solution (System Biosciences, LV810A) was added to the supernatant. The supernatant/PEG-*it* mixture was centrifuged at 1,500 g for 30 min at 4°C after refrigerated overnight. The supernatant was aspirated and the lentiviral pellet was resuspended in a small volume of RPMI-1640 medium. Aliquots of 10 μ l were stored at -80°C until ready for use.

For BMDMs and HMDMs infection, cells were incubated with lentiviral particles on day 4 at a multiplicity of infection (MOI) of 5 in RPMI-1640 medium complemented with 10% heated inactivated FBS (Gibco, 10270), 1% P/S, and 20–30% L929 culture supernatant. Cells were washed after 12 h and incubated in the regular growth medium. Cells were allowed to rest for 12 h, and a second infection was performed on day 5. Stimulations of lentivirus-infected cells were performed on day 8 after twice infections.

Inflammasome activation

Murine BMDMs were seeded in 24-well culture dishes and cultured overnight. All macrophages were primed for 4 h with 100 ng/ml ultrapure LPS (Sigma, L4774). NLRP3 activation was typically achieved as follows: 2 mM ATP (Invivogen, trl-atp) for 45 min; 10 μ M nigericin (Invivogen, trl-nig) for 1 h; 200 μ g/ml Alum (Invivogen, trl-alk), MSU (Invivogen, trl-msu) or Silica (Invivogen, trl-sio) for 6 h; 100 μ g/ml MDP (Invivogen, trl-mdp) for 12 h. Activation of the NLRC4 or AIM2 was achieved by transfection of 1 μ g/ml recombinant flagellin (Invivogen, trl-epstfla) using PULSIn (Polyplus-transfection, 501-01) and 1 μ g/ml Poly(dA:dT) (Invivogen, trl-patn-1) using Lipofectamine 3000 (Invitrogen, L3000015) for 12 h, respectively. Activation of the NLRP1 inflammasome was achieved by treatment for 16 h with anthrax lethal toxin (2.5 μ g/ml Anthrax Protective Antigen and 1 μ g/ml Anthrax Lethal Factor mix, List Biological Laboratories, 171D and 169A). The activation of NLRP3 inflammasome in HMDMs was achieved by treatments similar to those described above.

Western blot analysis

Cell lysates were prepared by direct lysis in 2 \times Laemmli sample buffer. To detect the secretion of caspase-1 p20, proteins in supernatants were concentrated by centrifugation at 12,000 g for 20 min at 4°C through a column with a cut-off of 10 kDa (Merk-Millipore). The protein samples were resolved on SDS-PAGE gels and transferred onto polyvinylidene difluoride (PVDF) membrane using a wet-transfer system. Membranes were blocked in 5% (wt/vol) non-fat milk in TBST (20 mM Tris-HCl, pH 7.6, 150 mM NaCl, and 0.1% (vol/vol) Tween-20) for 2 h at room temperature. Membranes were incubated with primary antibody diluted in 5% (wt/vol) non-fat milk in TBST at 4°C overnight. After being washed with TBST, the membrane was incubated with the appropriate horseradish peroxidase (HRP)-conjugated secondary antibody diluted in 5% (wt/vol) non-fat milk in TBST for 1 h. The resultant bands were visualized by the Chemiluminescence Western Blotting Detection system (Thermo Fisher Scientific) on X-ray films. Main primary antibodies used were as follows: rabbit monoclonal anti-NLRP3 (1:2,000, Cell Signaling Technology, 15101), mouse monoclonal anti-NLRP3 (1:1,000, Adipogen, AG-20B-0014), mouse monoclonal anti-mouse caspase-1

(1:500, Adipogen, AG-20B-0042), rabbit polyclonal anti-ASC (1:2,000, Adipogen, AG-25B-0006), goat polyclonal anti-mouse-IL-1 β (1:2,000, R&D Systems, AF-401-NA), rabbit polyclonal anti-ABRO1 (1:1,000, Bethyl Laboratories, A301-256A), rabbit monoclonal anti-BRCC3 (1:2,000, Cell Signaling Technology, 18215), rabbit monoclonal anti-BRE (1:2,000, Cell Signaling Technology, 12457), rabbit monoclonal anti-NBA1 (1:2,000, Cell Signaling Technology, 12711), mouse monoclonal anti-Ubiquitin (1:500, BostonBiochem, A-104), rabbit monoclonal anti-GAPDH (1:5,000, ABclonal, AC002), mouse monoclonal anti-Flag (1:4,000, Sigma, F3165), rabbit monoclonal anti-Flag (1:2,000, Cell Signaling Technology, 14793), mouse monoclonal anti-HA (1:1,000, Santa Cruz, sc-7392), and mouse monoclonal anti-Myc (1:2,000, ABclonal, AE010). Secondary HRP-conjugated antibodies used were goat anti-mouse IgG (1:5,000, Santa Cruz, sc-2005), goat anti-rabbit IgG (1:5,000, Santa Cruz, sc-2004), and bovine Anti-Goat IgG (1:2,000, Jackson Immuno-Research, 805-035-180).

Immunoprecipitation

The ubiquitination status of indicated proteins was detected as described (Choo & Zhang, 2009). If necessary, 10 μ M MG132 (MCE HY-13259) was added and incubated for 6 h. Cells were lysed in 100 μ l cell lysis buffer (2% SDS, 150 mM NaCl, 10 mM Tris-HCl, pH 8.0) with 10 mM N-ethylmaleimide and complete protease inhibitor mixture (Roche, 04693116001). Samples were boiled for 10 min, sheared with a sonication device, and then, 900 μ l dilution buffer (10 mM Tris-HCl, pH 8.0, 150 mM NaCl, 2 mM EDTA, 1% Triton) was added. After being incubated at 4°C for 30–60 min, the samples were centrifuged at 12,000 g for 30 min. The supernatants were incubated overnight at 4°C with anti-Flag M2 beads (Sigma, M8823) or anti-c-Myc agarose (Sigma, A7470), or for 4 h with appropriate antibody (1 μ g) followed by incubation with protein A/G agarose (Santa Cruz, sc-2003) for 6 h at 4°C. Immunoprecipitates were collected by centrifugation at 3,000 g for 3 min at 4°C, and the beads were then washed two times with 1 ml of washing buffer (10 mM Tris-HCl, pH 8.0, 1 M NaCl, 1 mM EDTA, 1% NP-40). An aliquot (40 μ l) of 2 \times Laemmli sample buffer was added to the beads. Immunoprecipitated samples were analyzed by immunoblot.

For co-immunoprecipitation (co-IP) assay, cells were lysed in 1 ml IP buffer (150 mM NaCl, 50 mM Tris-HCl, pH 8.0, 1% Triton X-100, 2 mM EDTA, complete protease inhibitor mixture [Roche]), sheared with a sonication device, and centrifuged at 12,000 g at 4°C for 30 min. Supernatants were then incubated with the appropriate antibody (1 μ g), anti-Flag M2 beads (Sigma, M8823), or anti-c-Myc agarose (Sigma, A7470) overnight at 4°C. An aliquot (50 μ l) of protein A/G agarose (Santa Cruz, sc-2003) was added to each sample when antibodies were used in the immunoprecipitation procedure, followed by incubation for 3 h at 4°C. Immunoprecipitates were collected by centrifugation at 3,000 g for 3 min at 4°C, and the beads were then washed four times with 1 ml of IP buffer. An aliquot (40 μ l) of 2 \times Laemmli sample buffer was added to the beads. Samples were resolved by SDS-PAGE.

Real-time PCR analysis

Total RNA was extracted by TRIzol (Invitrogen, 15596026). cDNA was generated from 2 μ g RNA using GoScript Reverse Transcription

System (Promega, A5000), and real-time PCR analyses were performed with SYBR Green Master Mix (TOYOBO, QPK-212) using the iQ5 Real-Time PCR Detection System (Bio-Rad). The mRNA level of target genes was normalized to that of the housekeeping gene *Gapdh*. Genes specific primers were designed by Primer Bank (Wang et al, 2012) and listed as follows:

Mouse *Gapdh* forward: 5'-AGGTCGGTGTGAACGGATTTG-3', and reverse: 5'-GGGGTCGTTGATGGCAACA-3';

Mouse *Il1b* forward: 5'-AAATACCTGTGGCCTTGGGC-3', and reverse: 5'-CTTGGGATCCACACTCTCCAG-3';

Mouse *Il6* forward: 5'-CTGCAAGAGACTTCCATCCAG-3'; and reverse: 5'-AGTGGTATAGACAGGTCTGTTGG-3';

Mouse *Tnfa* forward: 5'-FCTGAACTTCGGGGTGATCGG-3'; and reverse: 5'-GGCTTGCTACTCGAATTTTGA-3'.

Measurement of cytokines

Supernatants from cell culture, peritoneal lavage fluid, and serum were collected. Levels of indicated cytokines were determined using Cytometric bead array (CBA) Mouse IL-1 β Flex Set (BD Biosciences, 550232), Mouse TNF Flex Set (BD Biosciences, 558299), and Mouse IL-6 Flex Set (BD Biosciences, 558301), or analyzed with Mouse IL-1 β ELISA Kit (Abcam, ab197742), Human IL-1 β ELISA Kit (Abcam, ab214025), Mouse TNF- α ELISA Kit (Abcam, ab208348), and IL-18 Mouse ELISA Kit (Thermo Fisher Scientific, KMC0181) according to manufacturer's instructions.

Measurement of caspase-1 activity

LPS-primed BMDMs were loaded with FAM-YVAD-FMK (ImmunoChemistry, 98), fluorescent labeled probes for active caspase-1, prior to activation with 10 μ M nigericin. The intracellular caspase-1 activation was determined by flow cytometry on BD LSR Fortessa (BD Biosciences).

ASC oligomerization

ASC oligomerization assays were performed as previously described (Shenoy et al, 2012) with minor modifications. BMDMs were primed with LPS (100 ng/ml) for 4 h followed by 1-h nigericin (10 μ M) stimulation. Cells were washed with cold PBS and resuspended in an ice-cold buffer (20 mM HEPES-KOH, pH 7.5, 150 mM KCl, 5 mM EDTA, and protease inhibitor), and lysed by passing 20 times through a 21-G needle. Lysates were centrifuged at 900 g for 8 min to remove nuclei and unlysed cells. Supernatants were then centrifuged at 6,200 g for 8 min. The pellet fractions were washed twice with PBS and then cross-linked with 2 mM fresh Suberic acid bis (3-sulfo-N-hydroxysuccinimide ester) sodium salt (BS³, Sigma, 82436-77-9) for 1 h at 37°C and dissolved in SDS loading buffer to stop the cross-linking. The cross-linked pellets were separated in SDS-PAGE, and immunoblotting was performed.

Immunofluorescence

Bone marrow-derived macrophages were seeded on the glass bottom of 12-well plates and treated as described earlier. Cells were fixed in 4% paraformaldehyde for 15 min at room temperature. After two times wash with ice-cold PBS, cells were permeabilized

with 0.25% Triton X-100 for 15 min at room temperature. The cells were blocked with 5% BSA for 1 h at room temperature and then incubated with rabbit polyclonal anti-ASC (1:100) overnight at 4°C. After washing three times, cells were incubated Alexa Fluor 594-conjugated Goat anti-Rabbit IgG (1:1,000, Invitrogen, A-11012) secondary antibody for 1 h at room temperature. Nuclei were costained with Hoechst 33342. Images were acquired with a Zeiss LMS 710 confocal microscope. ASC specks were counted in five random areas of each image in triplicate experiments, and a minimum of 100 cells from each treatment condition were quantified.

Intracellular K⁺ and Ca²⁺ measurement

LPS-primed BMDMs were loaded with the K⁺-sensitive fluorescence indicator Asante Potassium Green-2 AM (APG-2, Abcam, ab142806) or Ca²⁺-sensitive fluorescence indicator Fluo-4 AM (Beyotime, S1060) prior to activation with 2 mM ATP for an additional 15 min. The intracellular K⁺ and Ca²⁺ levels were determined by flow cytometry on BD LSR Fortessa (BD Biosciences).

Mitochondrial ROS and Membrane potential analysis

LPS-primed BMDMs were stimulated with 10 μ M nigericin or 2 mM ATP for an additional 15 min and then incubated with 5 μ M MitoSOX red (Invitrogen, M36008) or 250 nM MitoTracker DeepRed FM (Invitrogen, M22426) for 15 min. Mitochondrial ROS and membrane potential were analyzed by flow cytometry on BD LSR Fortessa (BD Biosciences).

Cell viability analysis

Bone marrow-derived macrophages were seeded in 96-well plates and stimulated with ultrapure LPS (100 ng/ml) for indicated times. Cell viability was measured by the CellTiter-Glo Luminescent Cell Viability Assay (Promega, G7570).

In vivo induction of peritonitis

For induction of peritonitis, *Nlrp3*^{-/-}, *Abro1*^{-/-}, or *Brcc3*^{-/-} mice and age- and sex-matched normal control mice were injected intraperitoneally with Alum (1 mg) or MSU (1 mg) in 200 μ l PBS. After 6 h, peritoneal cavities were exudated with 5 ml of ice-cold PBS (with 5 mM EDTA). Peritoneal exudates were centrifuged at 800 g for 5 min. Cytokines in lavage fluids were detected by ELISA. Cells were stained and analyzed by flow cytometry.

In vivo LPS challenge

Abro1^{-/-} or *Brcc3*^{-/-} mice and age- and sex-matched normal control mice were injected intraperitoneally with LPS (15 mg/kg) (Sigma, L7011). The serum samples were collected after 3 h to detect serum cytokine levels. For lethality, mice were monitored for 9 days.

Flow cytometry

Peritoneal cell exudates were washed in PBS and incubated with Fixable Viability Dye eFluor 780 (eBioscience, 65-0865) for 30 min.

Surface stains for anti-CD45-FITC (eBioscience, 11-0451), anti-CD11b-eFluor450 (eBioscience, 48-0112), anti-Ly6C-PE-Cy7 (eBioscience, 25-5932), and anti-Ly6G-APC (eBioscience, 17-9668) were added and incubated for an additional 30 min. Cells were gated first on live CD45⁺ cells. Inflammatory monocytes and neutrophils were identified as CD45⁺CD11b⁺Ly6G⁻Ly6C⁺ and CD45⁺CD11b⁺Ly6G⁺Ly6C⁻, respectively. The number of leukocytes (CD45⁺ cells) was counted by 123-count eBeads Counting Beads (eBioscience, 01-1234). Acquisition was performed on a BD LSRFortessa (BD Biosciences) with a minimum of 10,000 target cells collected, and marker expression was examined using the FACSDiva v7.0 software (BD Biosciences). Data were also further analyzed using FlowJo v10.0 (FlowJo, LLC).

Statistical analyses

Statistics were calculated with GraphPad Prism 7 (GraphPad Software). Data are expressed as means \pm SEM. Statistical tests were selected based on appropriate assumptions with respect to data distribution and variance characteristics. The distribution of variables is tested by the Kolmogorov–Smirnov test. The variance was similar in the groups being compared. Statistical analysis was carried out using a standard two-tailed unpaired Student's *t*-test for single comparisons, one- or two-way ANOVA for multiple comparisons, and a log-rank (Mantel-Cox) test for survival analysis. *P*-values < 0.05 were deemed statistically significant. The data reported are representative of at least three experiments. All *P*-values are shown in Appendix Table S1.

Data availability

The data that support the findings of this study are available from the corresponding author on reasonable request.

Expanded View for this article is available online.

Acknowledgements

We thank Dr. Tao Li (National Center of Biomedical Analysis, China) for providing NLRP3 mutant plasmids, *Nlrp3*^{S194A/S194A} BMDMs, *Nlrp3*^{-/-} mice, and his helpful discussion; Dr. Jian Wang (Beijing Proteome Research Center, China) for providing human NLRP3, pro-caspase-1, pro-IL-1 β plasmids. This work was supported by grants from the Major State Basic Research of China (2013CB910800); the National Key Research and Development Program of China (2016YFA0100600); the State Key Laboratory of Proteomics (SKLP-K201404); and the National Natural Science Foundation of China (31301124).

Author contributions

GR, RY, XZ, YX, WZ, YW, WM, XW, PS, LL, HC, YZ, JZ, MY, CG, and CL performed the experiments for this work; GR contributed all *in vitro* and *in vivo* experiments; GR, XZ, and YX contributed *in vitro* experiments and assisted by WM, XW, and JZ; GR, RY, YX performed murine *in vivo* experiments and assisted by WZ, YW, PS, LL, MY, CG, and CL; HC and YZ contributed mice or reagents. RY and GR designed the experiments. RY and GR analyzed the data. XY, RY, and GR wrote the manuscript. XY and RY supervised the project.

Conflict of interest

The authors declare that they have no conflict of interest.

References

- Abderrazak A, Syrovets T, Couchie D, El Hadri K, Friguet B, Simmet T, Rouis M (2015) NLRP3 inflammasome: from a danger signal sensor to a regulatory node of oxidative stress and inflammatory diseases. *Redox Biol* 4: 296–307
- Baker PJ, De Nardo D, Moghaddas F, Tran LS, Bachem A, Nguyen T, Hayman T, Tye H, Vince JE, Bedoui S, Ferrero RL, Masters SL (2017) Posttranslational modification as a critical determinant of cytoplasmic innate immune recognition. *Physiol Rev* 97: 1165–1209
- Baroja-Mazo A, Martin-Sanchez F, Gomez AI, Martinez CM, Amores-Iniesta J, Compan V, Barbera-Cremades M, Yague J, Ruiz-Ortiz E, Anton J, Bujan S, Couillin I, Brough D, Arostegui JI, Pelegrin P (2014) The NLRP3 inflammasome is released as a particulate danger signal that amplifies the inflammatory response. *Nat Immunol* 15: 738–748
- Bauernfeind FG, Horvath G, Stutz A, Alnemri ES, MacDonald K, Speert D, Fernandes-Alnemri T, Wu J, Monks BG, Fitzgerald KA, Hornung V, Latz E (2009) Cutting edge: NF- κ B activating pattern recognition and cytokine receptors license NLRP3 inflammasome activation by regulating NLRP3 expression. *J Immunol* 183: 787–791
- Cai X, Chen J, Xu H, Liu S, Jiang QX, Halfmann R, Chen ZJ (2014) Prion-like polymerization underlies signal transduction in antiviral immune defense and inflammasome activation. *Cell* 156: 1207–1222
- Choo YS, Zhang Z (2009) Detection of protein ubiquitination. *J Vis Exp* 30: e1293
- Coll RC, Robertson AA, Chae JJ, Higgins SC, Munoz-Planillo R, Inserra MC, Vetter I, Dungan LS, Monks BG, Stutz A, Croker DE, Butler MS, Haneklaus M, Sutton CE, Nunez G, Latz E, Kastner DL, Mills KH, Masters SL, Schroder K et al (2015) A small-molecule inhibitor of the NLRP3 inflammasome for the treatment of inflammatory diseases. *Nat Med* 21: 248–255
- Cooper EM, Cutcliffe C, Kristiansen TZ, Pandey A, Pickart CM, Cohen RE (2009) K63-specific deubiquitination by two JAMM/MPN+ complexes: BRISC-associated Brcc36 and proteasomal Poh1. *EMBO J* 28: 621–631
- Feng L, Wang J, Chen J (2010) The Lys63-specific deubiquitinating enzyme BRCC36 is regulated by two scaffold proteins localizing in different subcellular compartments. *J Biol Chem* 285: 30982–30988
- Fernandes-Alnemri T, Wu J, Yu JW, Datta P, Miller B, Jankowski W, Rosenberg S, Zhang J, Alnemri ES (2007) The pyroptosome: a supramolecular assembly of ASC dimers mediating inflammatory cell death via caspase-1 activation. *Cell Death Differ* 14: 1590–1604
- Fernandes-Alnemri T, Kang S, Anderson C, Sagara J, Fitzgerald KA, Alnemri ES (2013) Cutting edge: TLR signaling licenses IRAK1 for rapid activation of the NLRP3 inflammasome. *J Immunol* 191: 3995–3999
- Franchi L, Eigenbrod T, Munoz-Planillo R, Nunez G (2009) The inflammasome: a caspase-1-activation platform that regulates immune responses and disease pathogenesis. *Nat Immunol* 10: 241–247
- Gattorno M, Tassi S, Carta S, Delfino L, Ferlito F, Pelagatti MA, D'Osualdo A, Buoncompagni A, Alpigiani MG, Alessio M, Martini A, Rubartelli A (2007) Pattern of interleukin-1 β secretion in response to lipopolysaccharide and ATP before and after interleukin-1 blockade in patients with CIAS1 mutations. *Arthritis Rheum* 56: 3138–3148
- Guo C, Xie S, Chi Z, Zhang J, Liu Y, Zhang L, Zheng M, Zhang X, Xia D, Ke Y, Lu L, Wang D (2016) Bile acids control inflammation and metabolic disorder through inhibition of NLRP3 inflammasome. *Immunity* 45: 802–816
- Han S, Lear TB, Jerome JA, Rajbhandari S, Snavelly CA, Gulick DL, Gibson KF, Zou C, Chen BB, Mallampalli RK (2015) Lipopolysaccharide primes the NALP3 inflammasome by inhibiting its ubiquitination and degradation mediated by the SCFFBXL2 E3 ligase. *J Biol Chem* 290: 18124–18133

- Harrigan JA, Jacq X, Martin NM, Jackson SP (2018) Deubiquitylating enzymes and drug discovery: emerging opportunities. *Nat Rev Drug Discovery* 17: 57–78
- He Y, Hara H, Nunez G (2016) Mechanism and regulation of NLRP3 inflammasome activation. *Trends Biochem Sci* 41: 1012–1021
- Hu X, Kim JA, Castillo A, Huang M, Liu J, Wang B (2011) NBA1/MERIT40 and BRE interaction is required for the integrity of two distinct deubiquitinating enzyme BRCC36-containing complexes. *J Biol Chem* 286: 11734–11745
- Huai W, Zhao R, Song H, Zhao J, Zhang L, Zhang L, Gao C, Han L, Zhao W (2014) Aryl hydrocarbon receptor negatively regulates NLRP3 inflammasome activity by inhibiting NLRP3 transcription. *Nat Commun* 5: 4738
- Jiang H, He H, Chen Y, Huang W, Cheng J, Ye J, Wang A, Tao J, Wang C, Liu Q, Jin T, Jiang W, Deng X, Zhou R (2017) Identification of a selective and direct NLRP3 inhibitor to treat inflammatory disorders. *J Exp Med* 214: 3219–3238
- Jin J, Yu Q, Han C, Hu X, Xu S, Wang Q, Wang J, Li N, Cao X (2013) LRRFIP2 negatively regulates NLRP3 inflammasome activation in macrophages by promoting Flightless-I-mediated caspase-1 inhibition. *Nat Commun* 4: 2075
- Juliana C, Fernandes-Alnemri T, Kang S, Farias A, Qin F, Alnemri ES (2012) Non-transcriptional priming and deubiquitination regulate NLRP3 inflammasome activation. *J Biol Chem* 287: 36617–36622
- Kanneganti TD, Lamkanfi M (2013) K(+) drops tilt the NLRP3 inflammasome. *Immunity* 38: 1085–1088
- Kim M-J, Yoon J-H, Ryu J-H (2016) Mitophagy: a balance regulator of NLRP3 inflammasome activation. *BMB Rep* 49: 529–535
- Lopez-Castejon G, Luheshi NM, Compan V, High S, Whitehead RC, Flitsch S, Kirov A, Prudovsky I, Swanton E, Brough D (2013) Deubiquitinases regulate the activity of caspase-1 and interleukin-1beta secretion via assembly of the inflammasome. *J Biol Chem* 288: 2721–2733
- Mariathasan S, Weiss DS, Newton K, McBride J, O'Rourke K, Roose-Girma M, Lee WP, Weinrauch Y, Monack DM, Dixit VM (2006) Cryopyrin activates the inflammasome in response to toxins and ATP. *Nature* 440: 228–232
- Masters SL, Simon A, Aksentjevich I, Kastner DL (2009) Horror autinflammaticus: the molecular pathophysiology of autoinflammatory disease (*). *Annu Rev Immunol* 27: 621–668
- Menu P, Vince JE (2011) The NLRP3 inflammasome in health and disease: the good, the bad and the ugly. *Clin Exp Immunol* 166: 1–15
- Palazon-Riquelme P, Worboys JD, Green J, Valera A, Martin-Sanchez F, Pellegrini C, Brough D, Lopez-Castejon G (2018) USP7 and USP47 deubiquitinases regulate NLRP3 inflammasome activation. *EMBO Rep* 19: e44766
- Ply BF, Kim M-S, Vakifahmetoglu-Norberg H, Yuan J (2013) Deubiquitination of NLRP3 by BRCC3 critically regulates inflammasome activity. *Mol Cell* 49: 331–338
- Schroder K, Tschopp J (2010) The inflammasomes. *Cell* 140: 821–832
- Shenoy AR, Wellington DA, Kumar P, Kassa H, Booth CJ, Cresswell P, MacMicking JD (2012) GBP5 promotes NLRP3 inflammasome assembly and immunity in mammals. *Science* 336: 481–485
- Song H, Liu B, Huai W, Yu Z, Wang W, Zhao J, Han L, Jiang G, Zhang L, Gao C, Zhao W (2016) The E3 ubiquitin ligase TRIM31 attenuates NLRP3 inflammasome activation by promoting proteasomal degradation of NLRP3. *Nat Commun* 7: 13727
- Song N, Liu ZS, Xue W, Bai ZF, Wang QY, Dai J, Liu X, Huang YJ, Cai H, Zhan XY, Han QY, Wang H, Chen Y, Li HY, Li AL, Zhang XM, Zhou T, Li T (2017) NLRP3 phosphorylation is an essential priming event for inflammasome activation. *Mol Cell* 68: 185–197.e186
- Stutz A, Kolbe CC, Stahl R, Horvath GL, Franklin BS, van Ray O, Brinkschulte R, Geyer M, Meissner F, Latz E (2017) NLRP3 inflammasome assembly is regulated by phosphorylation of the pyrin domain. *J Exp Med* 214: 1725–1736
- Subramanian N, Natarajan K, Clatworthy MR, Wang Z, Germain RN (2013) The adaptor MAVS promotes NLRP3 mitochondrial localization and inflammasome activation. *Cell* 153: 348–361
- de Torre-Minguela C, Mesa Del Castillo P, Pelegrin P (2017) The NLRP3 and pyrin inflammasomes: implications in the pathophysiology of autoinflammatory diseases. *Front Immunol* 8: 43
- Tripathi E, Smith S (2017) Cell cycle-regulated ubiquitination of tankyrase 1 by RNF8 and ABRO1/BRCC36 controls the timing of sister telomere resolution. *EMBO J* 36: 503–519
- Tschopp J, Schroder K (2010) NLRP3 inflammasome activation: the convergence of multiple signalling pathways on ROS production? *Nat Rev Immunol* 10: 210–215
- Vanden Berghe T, Demon D, Bogaert P, Vandendriessche B, Goethals A, Depuydt B, Vuylsteke M, Roelandt R, Van Wonterghem E, Vandembroecke J, Choi SM, Meyer E, Krautwald S, Declercq W, Takahashi N, Cauwels A, Vandenaebroeck P (2014) Simultaneous targeting of IL-1 and IL-18 is required for protection against inflammatory and septic shock. *Am J Respir Crit Care Med* 189: 282–291
- Wang B, Matsuoka S, Ballif BA, Zhang D, Smogorzewska A, Gygi SP, Elledge SJ (2007) Abraxas and RAP80 form a BRCA1 protein complex required for the DNA damage response. *Science* 316: 1194–1198
- Wang X, Spandidos A, Wang H, Seed B (2012) PrimerBank: a PCR primer database for quantitative gene expression analysis, 2012 update. *Nucleic Acids Res* 40: D1144–D1149
- Xu M, Moresco JJ, Chang M (2018) SHMT2 and the BRCC36/BRISC deubiquitinase regulate HIV-1 Tat K63-ubiquitylation and destruction by autophagy. *PLoS Pathog* 14: e1007071
- Yan K, Li L, Wang X, Hong R, Zhang Y, Yang H, Lin M, Zhang S, He Q, Zheng D, Tang J, Yin Y, Shao G (2015a) The deubiquitinating enzyme complex BRISC is required for proper mitotic spindle assembly in mammalian cells. *J Cell Biol* 210: 209–224
- Yan Y, Jiang W, Liu L, Wang X, Ding C, Tian Z, Zhou R (2015b) Dopamine controls systemic inflammation through inhibition of NLRP3 inflammasome. *Cell* 160: 62–73
- Zhang X, Goncalves R, Mosser DM (2008) The isolation and characterization of murine macrophages. *Curr Protoc Immunol* Chapter 14: Unit 14 11
- Zheng H, Gupta V, Patterson-Fortin J, Bhattacharya S, Katlinski K, Wu J, Varghese B, Carbone CJ, Aressy B, Fuchs SY, Greenberg RA (2013) A BRISC-SHMT complex deubiquitinates IFNAR1 and regulates interferon responses. *Cell Rep* 5: 180–193